# High energy state interactions, energetics and multiphoto-fragmentation processes of HI

**Meng-Xu Jiang and Ágúst Kvaran***

*Science Institute, University of Iceland, Dunhagi 3, 107 Reykjavík, Iceland.*

**Supplementary material:** Supporting material (figures and tables) to go with the main text of the paper " High energy state interactions, energetics and multiphoto-fragmentation processes of HI"

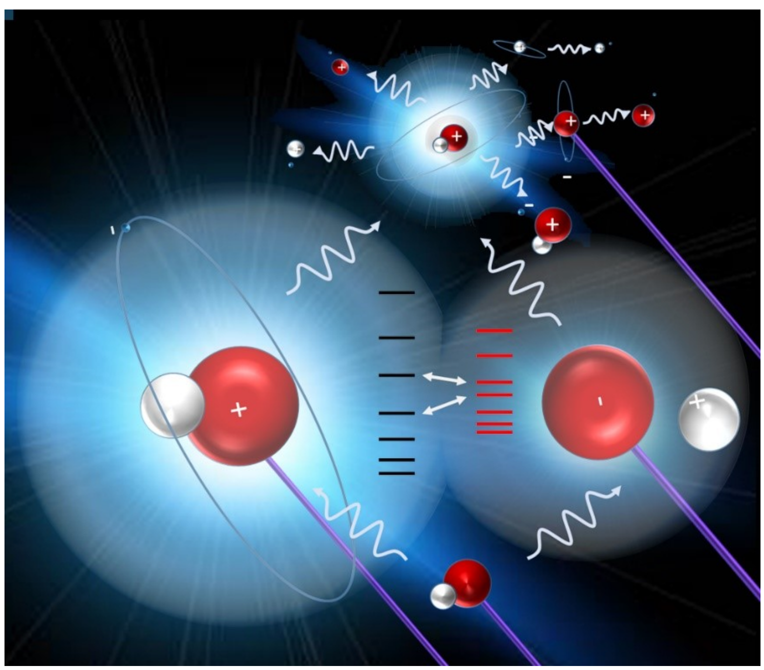

**Content:** **pages:**

## Figures:

## Tables:

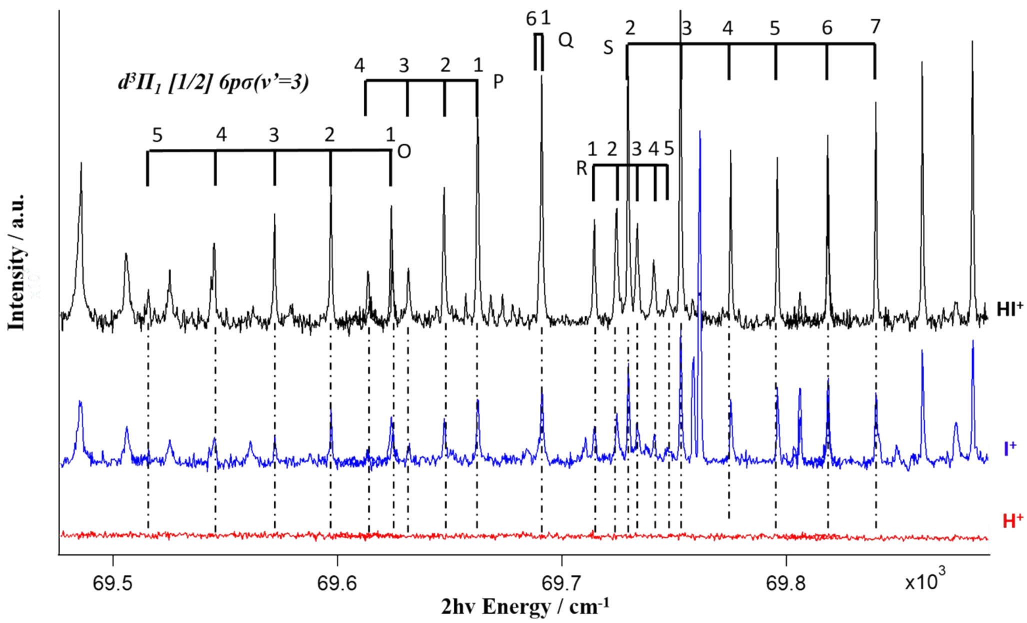


**Fig. S1 a)** REMPI spectra for HI for 2hν resonant transition in the excitation region of 69480 – 69900 cm-1. Top (black) is the $HI^+$ ion, middle (blue) is $I^+$ ion, bottom (red) is $H^+$ ion. The new $d^3\Pi_1$ [3/2] 6pσ($v'$=3) Rydberg states was located and assigned in the $HI^+$ and $I^+$ spectra.

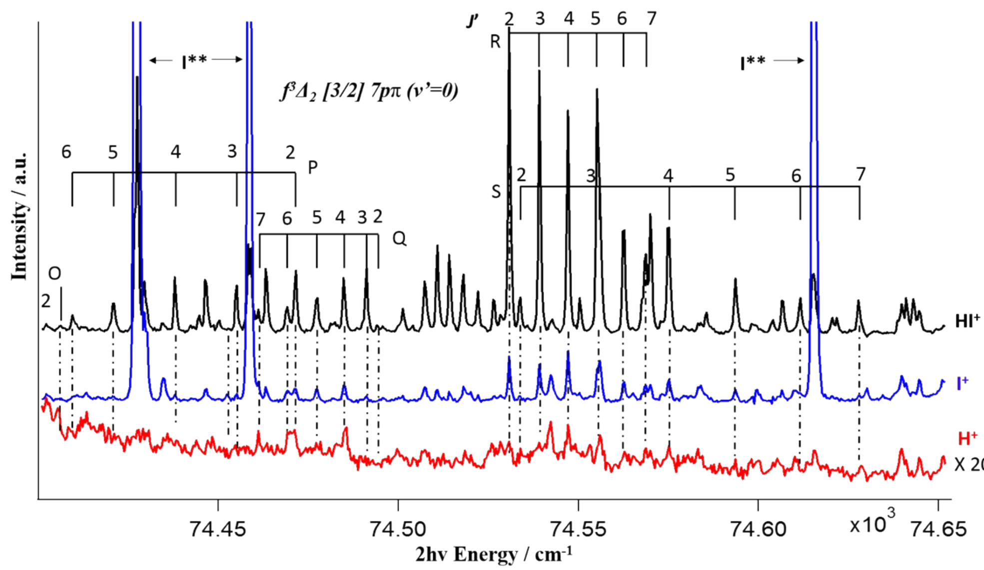


**Fig. S1 b)** REMPI spectra for HI due to 2hν resonance transition in the energy region of 74 440 – 74 620 cm-1. Ions are indicated. Assignment of rotational line of the $F^1\Delta_2$ [1/2] 6pπ ($v'$=2) Rydberg state spectrum in the $HI^+$ ion spectrum is shown.

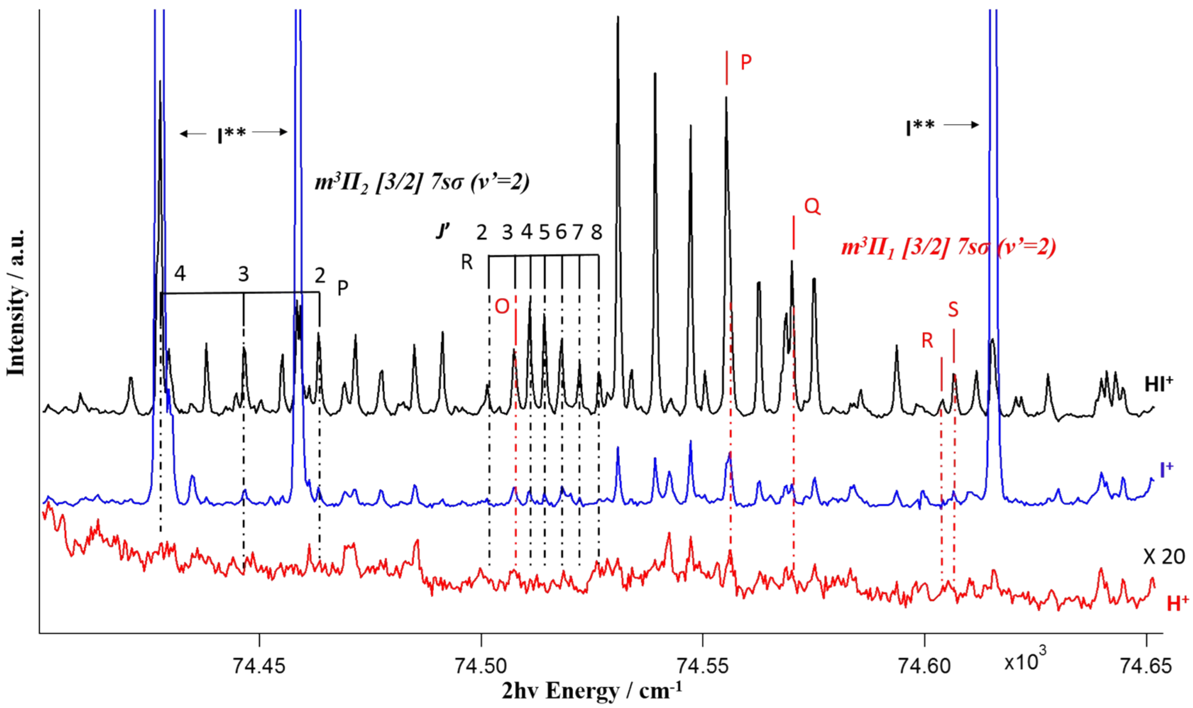


**Fig. S1 c)** REMPI spectra of HI due to 2hν resonance transition in the excitation region of 74 440 – 74 620 $cm^{-1}$. Assignment of rotational line of the $m^3\Pi_{2,1}[1/2]7s\sigma$ ($v'$=2) Rydberg state spectrum in the $HI^+$ ion spectrum is indicated.

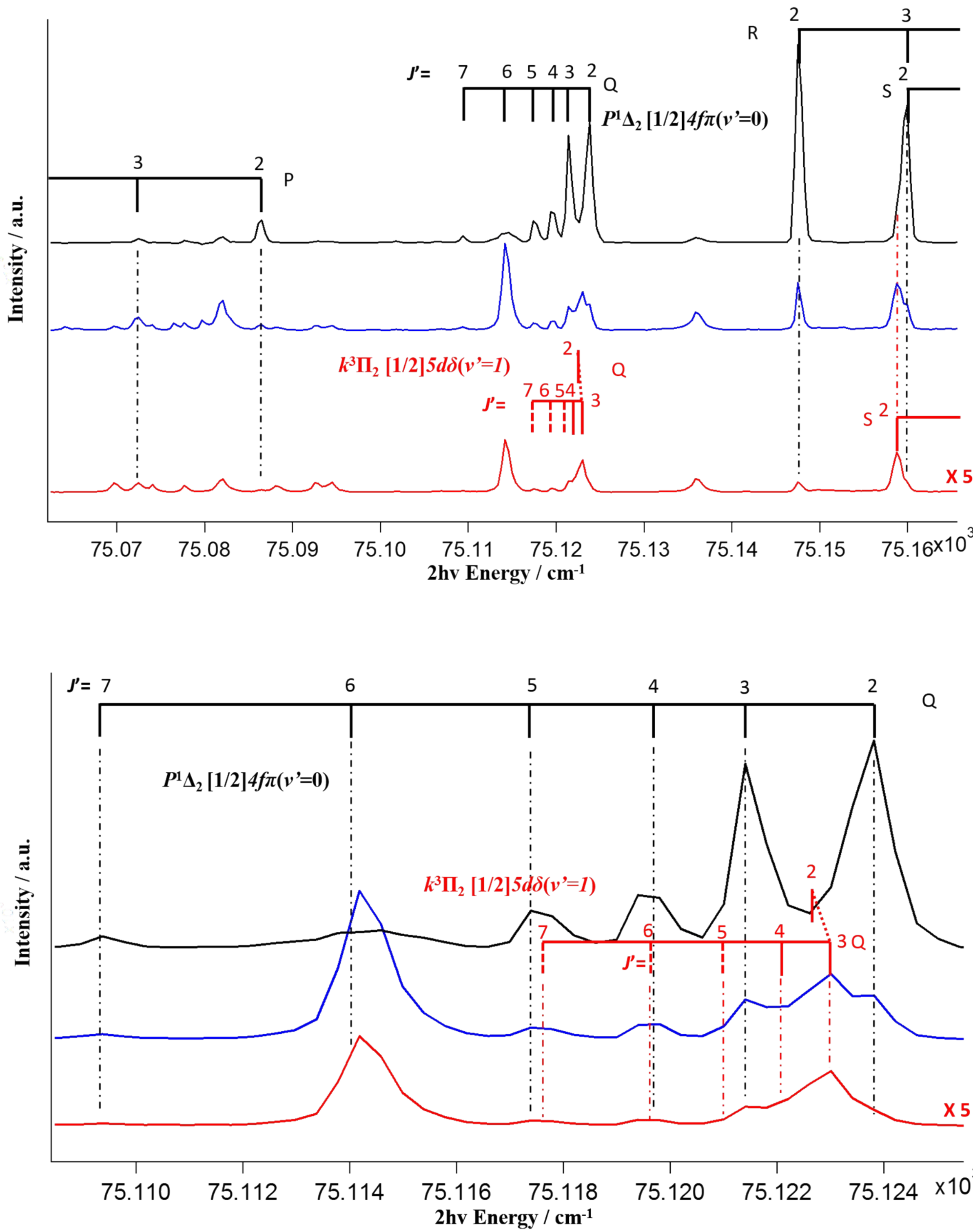


**Fig S2 a)** REMPI spectra for HI due to 2hν resonance transition in the excitation region of 75000 – 75200 cm$^{-1}$. Top (black): $HI^+$ ion, middle (blue): $I^+$ ion, bottom (red): $H^+$ ion. The new $k^3\Pi_2$ [1/2]5d$\delta$($v'$=1) Rydberg state spectrum was located and assigned.

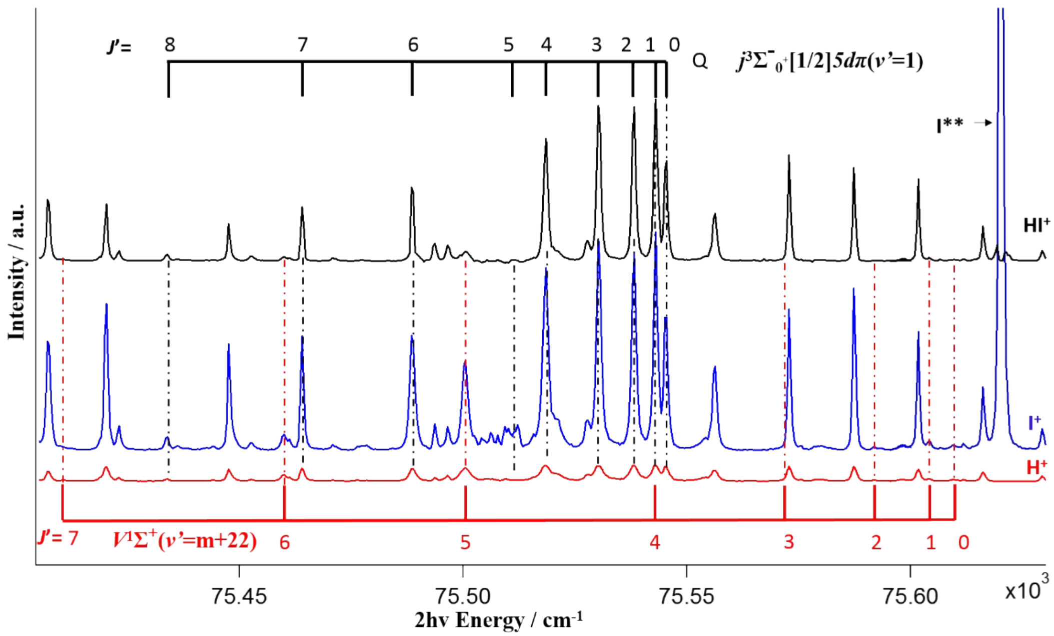


**Fig. S2 b)** REMPI spectra for HI due to 2hν resonance transition in the excitation region of 75300 – 75700 cm$^{-1}$. Assignment of rotational $Q$-lines, $J'$ = 0 -7 for the $V^1\Sigma^+(v' = m + 22)$ ion-pair vibrational state in the $I^+$ and $H^+$ ion spectrum is shown.

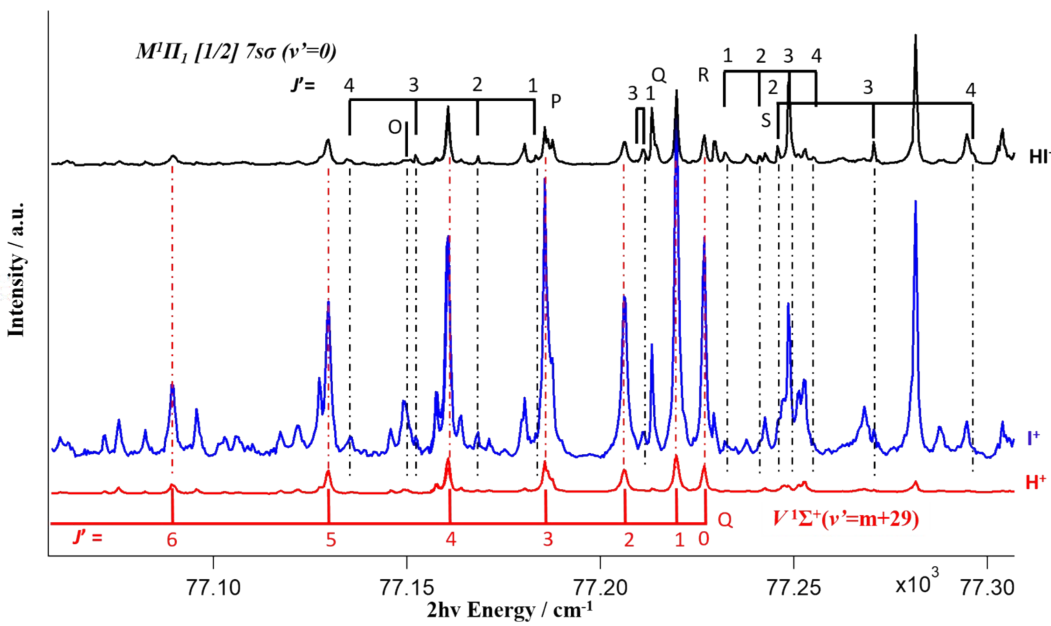


**Fig. S2 c)** REMPI spectra for HI due to 2hν resonance transition in the excitation region of 77000 – 77300cm$^{-1}$. Ions are indicated. The new $M^1\Pi_1$ [1/2]7s$\sigma$($v'$=0) Rydberg state spectrum was located and assigned.

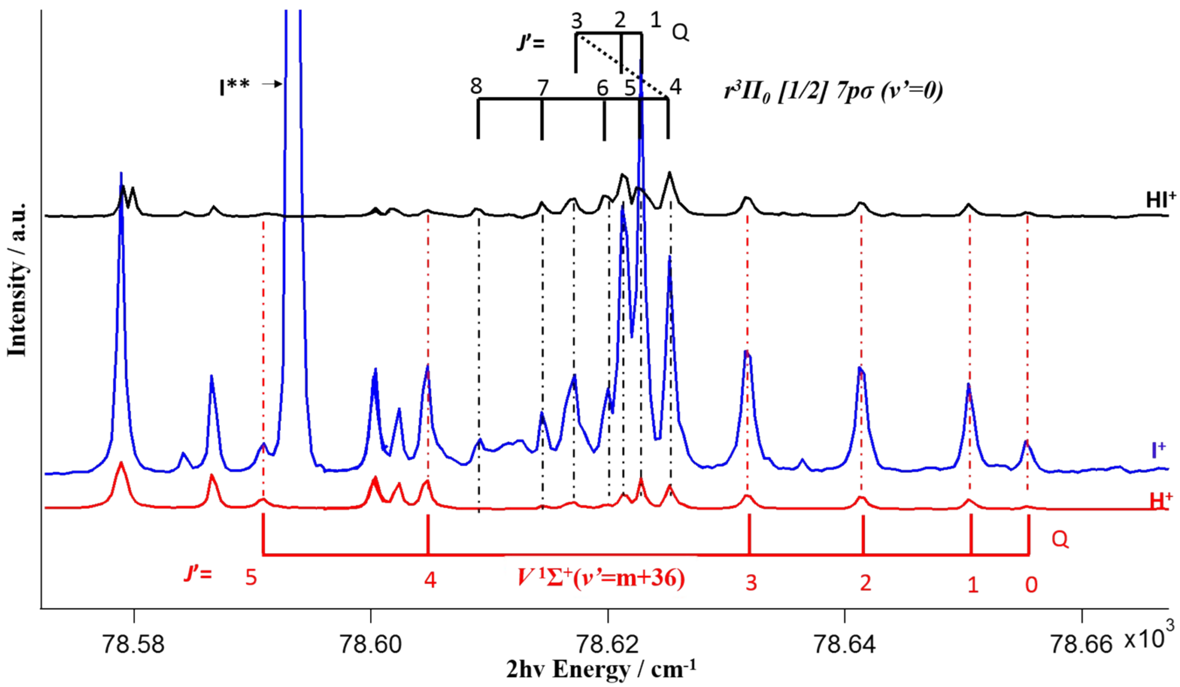


**Fig. S2 d)** REMPI spectra for HI due to 2hν resonance transition in the excitation region of 78500 – 78700 cm$^{-1}$. Top (black): $HI^+$ ion, middle (blue): $I^+$ ion, bottom (red): $H^+$ ion. The new $R^1\Pi_1$ [1/2]7p$\sigma$($v'$=0) Rydberg state spectrum and $V^1\Sigma^+$($v'$=$m$+36) ) ion-paired state spectrum were located and assigned.

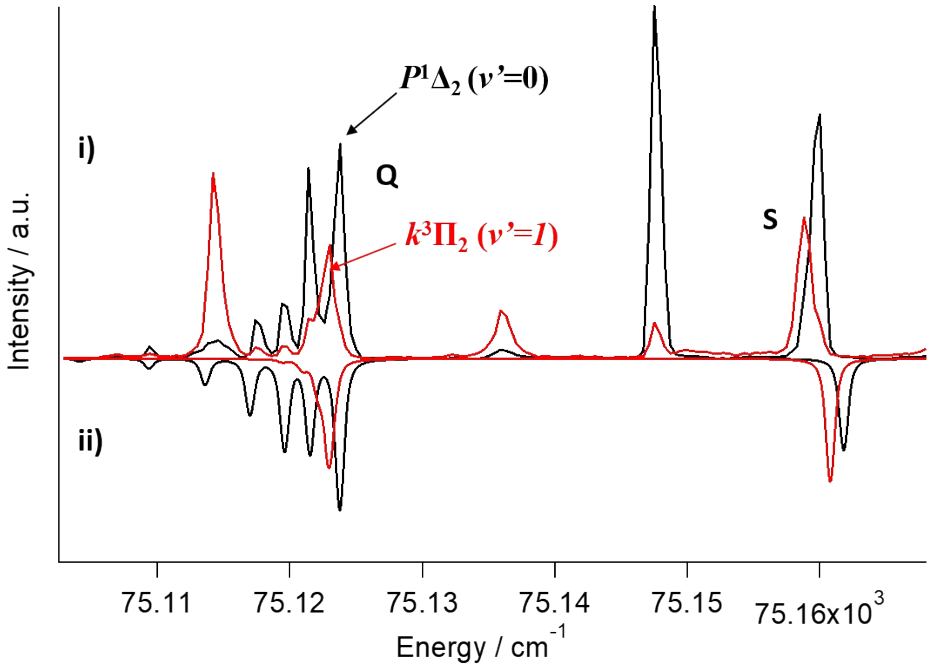


**Fig. S3 a)** Simulation of $P^1\Delta_2$ [1/2]4f$\pi$($v'$=0) and $k^3\Pi_2$ [1/2]5d$\delta$($v'$=1) system, i) Experimental data; ii) calculated.

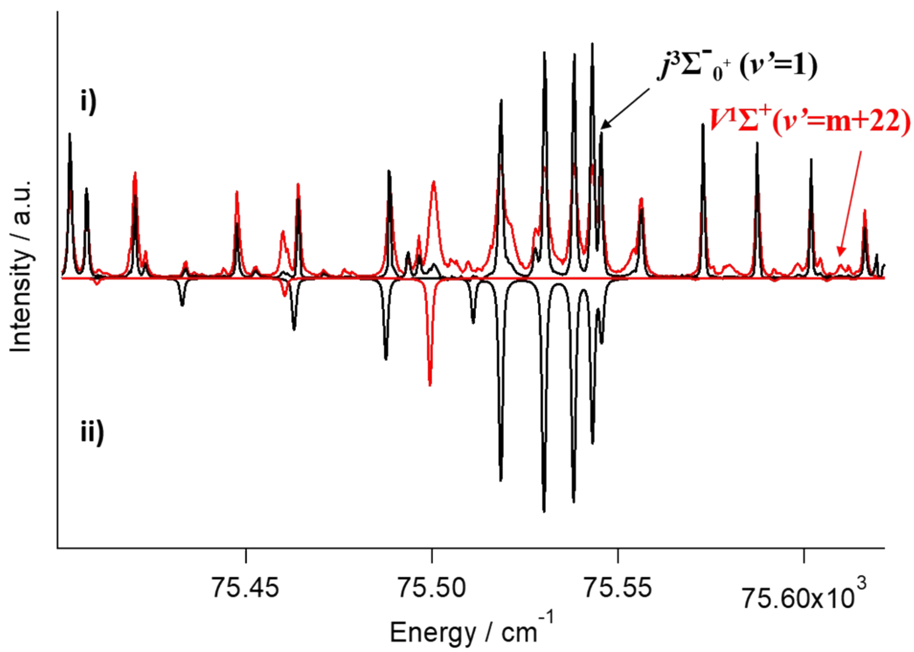


**Fig. S3 b)** Simulation of $j^3\Sigma^-_0{}^+$[1/2]5d$\pi$($v'$=1) and $V^1\Sigma^+$($v'$=$m$+22) system, i) Experimental data; ii) calculated.

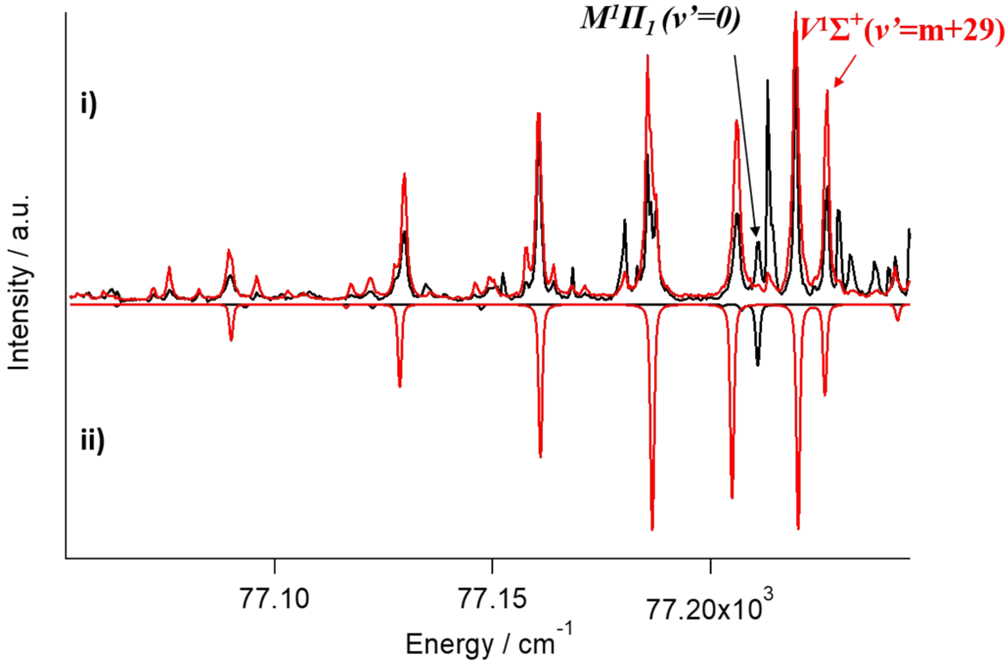


**Fig. S3 c)** Simulation of $M^1\Pi_1$ [1/2]7s$\sigma$($v'$=0) and $V^1\Sigma^+$($v'$=$m$+29) system, i) Experimental data; ii) calculated.

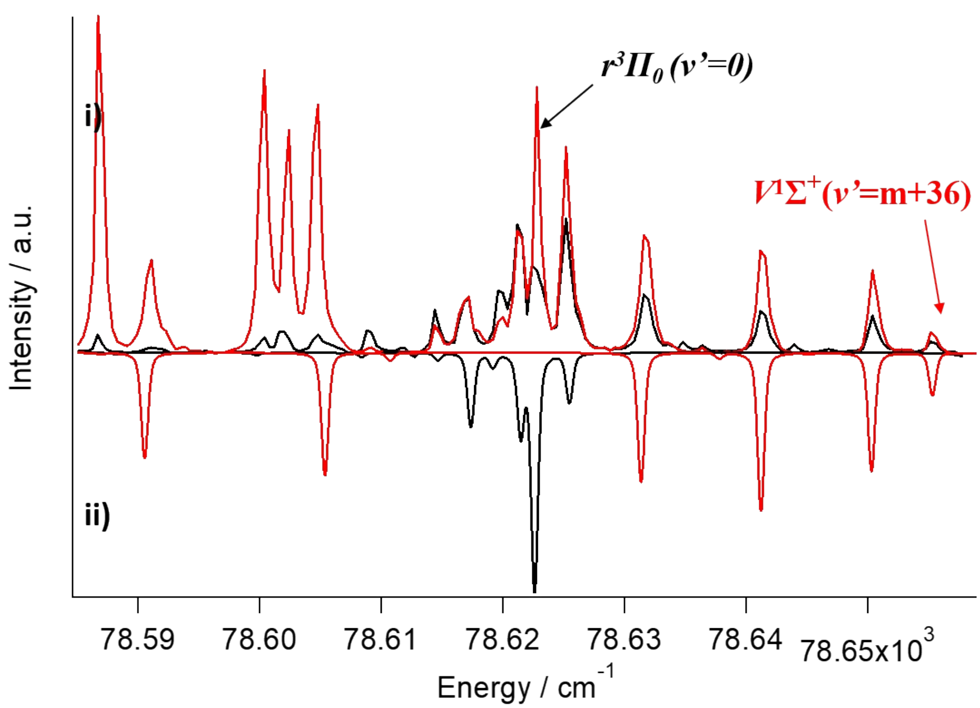


**Fig. S3 d)** Simulation of $r^3\Pi_0$ [1/2]7p$\sigma$($v'$=0) and $V^1\Sigma^+$($v'$=$m$+36) system, i) Experimental data; ii) calculated.

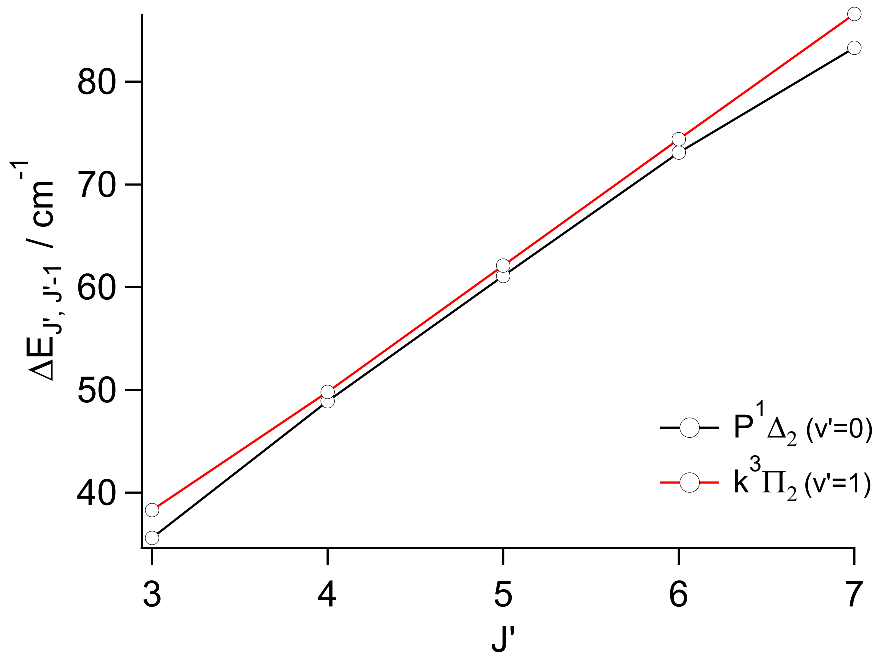


**Fig. S4 a)** Perturbation effects due to the $P^1\Delta_2$ [1/2]4f$\pi$($v'$=0) and $k^3\Pi_2$ [1/2]5d$\delta$($v'$=1) state interaction. Spacing between rotational levels ($\Delta E_{J,\,J\text{-}1}$) as a function of $J'$; experimental values

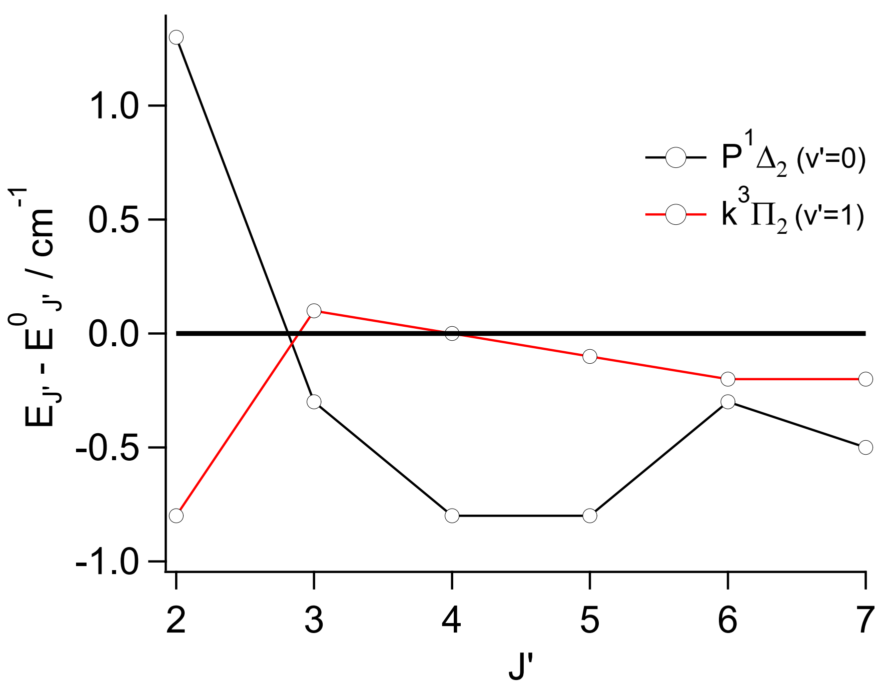


**Fig.S4 b)** Perturbation effects due to the $P^1\Delta_2$ [1/2]4f$\pi$($v'$=0) and $k^3\Pi_2$ [1/2]5d$\delta$($v'$=1) state interaction. Reduced term value plots: Deperturbed energy level values subtracted from experimental energy level values

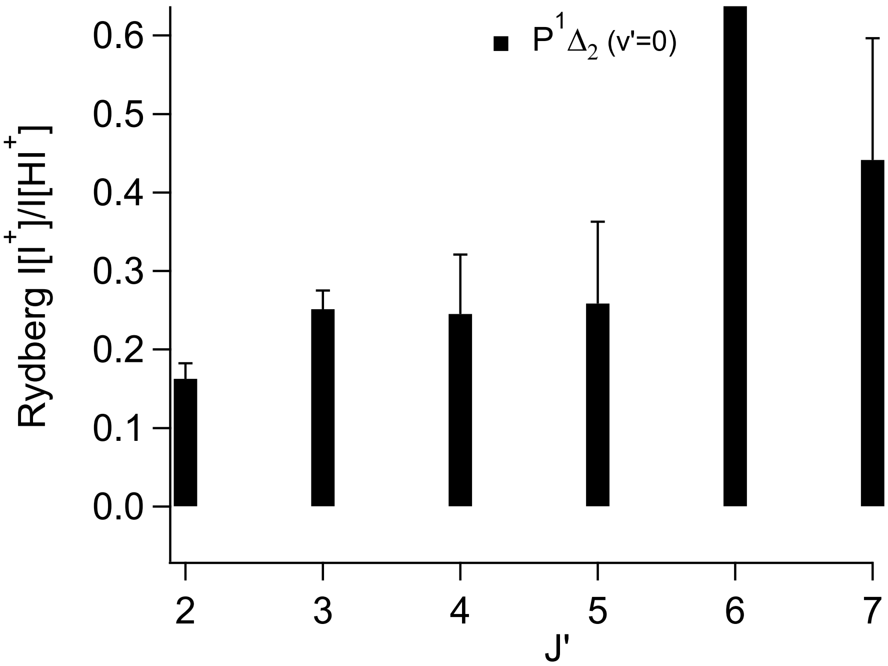


**Fig. S4 c)** Perturbation effects due to the $P^1\Delta_2$ [1/2]4f$\pi$($v'$=0) and $k^3\Pi_2$ [1/2]5d$\delta$($v'$=1) state interaction. Relative ion-signal intensities ($I$($I^+$ )/$I$($HI^+$ )) vs. $J'$ derived from the $Q$-rotational lines for the $P^1\Delta_2$ [1/2]4f$\pi$($v'$=0) spectrum.

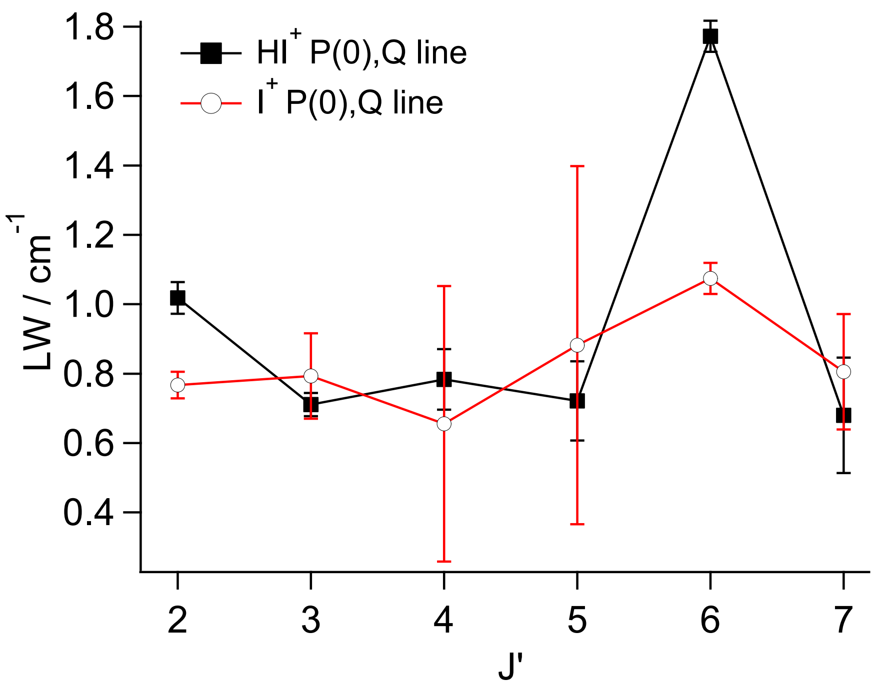


**Fig. S4 d)** Perturbation effects due to the $P^1\Delta_2$ [1/2]4f$\pi$($v'$=0) and $k^3\Pi_2$ [1/2]5d$\delta$($v'$=1) state interaction. Rotational line-widths vs $J'$ derived from the $Q$ lines of the $I^+$ signals for the $P^1\Delta_2$ [1/2]4f$\pi$($v'$=0) state spectrum.

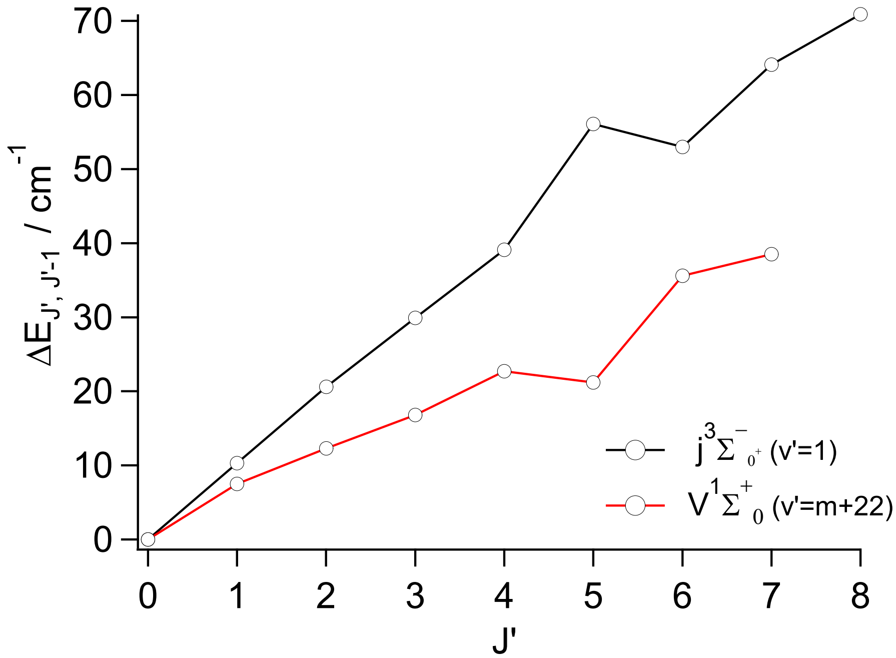


**Fig. S5 a)** Perturbation effects due to the $j^3\Sigma^-_0{}^+[1/2]5d\pi(v'=1)$ and $V^1\Sigma^+(v'=m+22)$ state interaction. Spacing between rotational levels ($\Delta E_{J, J-1}$) as a function of $J'$.

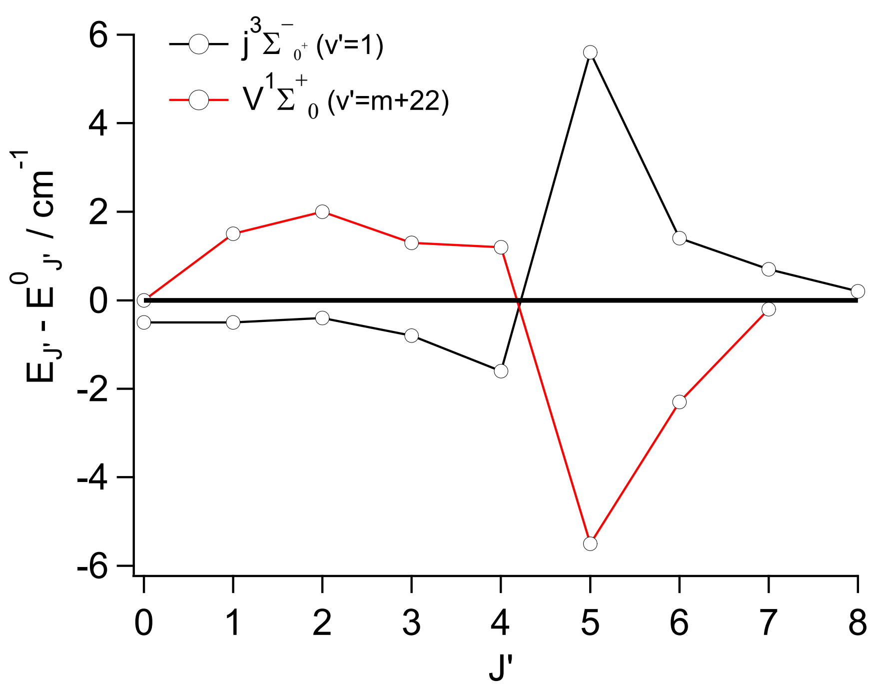


**Fig. S5 b)** Perturbation effects due to the $j^3\Sigma^-_0{}^+[1/2]5d\pi(v'=1)$ and $V^1\Sigma^+(v'=m+22)$ state interaction. Reduced term value plots: Deperturbed energy level values subtracted from experimental energy level values.

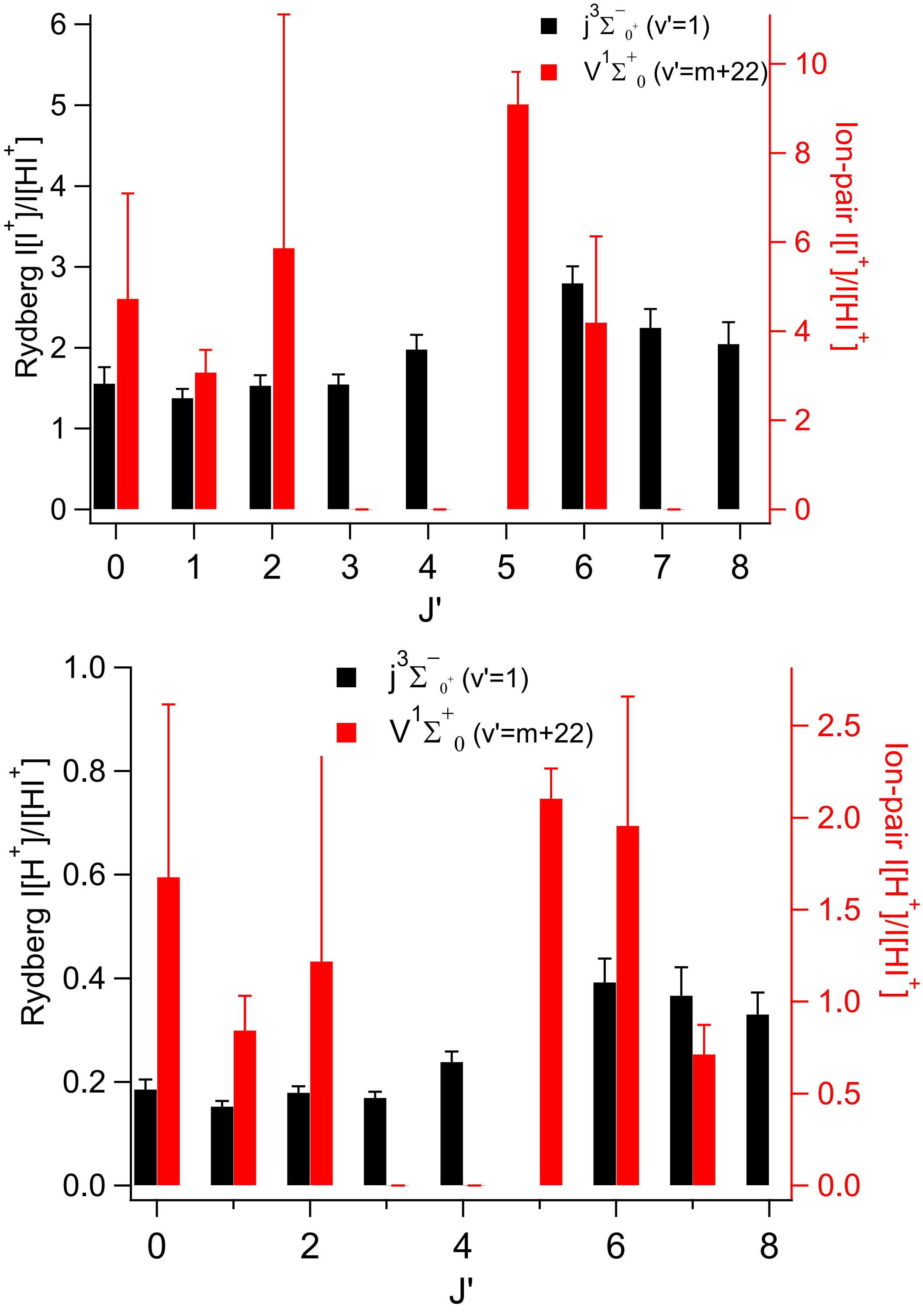


**Fig. S5 c)** Perturbation effects due to the $j^3\Sigma^-_0{}^+[1/2]5d\pi(v'=1)$ and $V^1\Sigma^+(v'=m+22)$ state interaction. Relative ion-signal intensities ($I(I^+)/I(HI^+)$ and $I(H^+)/I(HI^+)$) vs. $J'$ derived from the $Q$-rotational lines for the $j^3\Sigma^-_0{}^+[1/2]5d\pi(v'=1)$ and $V^1\Sigma^+(v'=m+22)$ spectra.

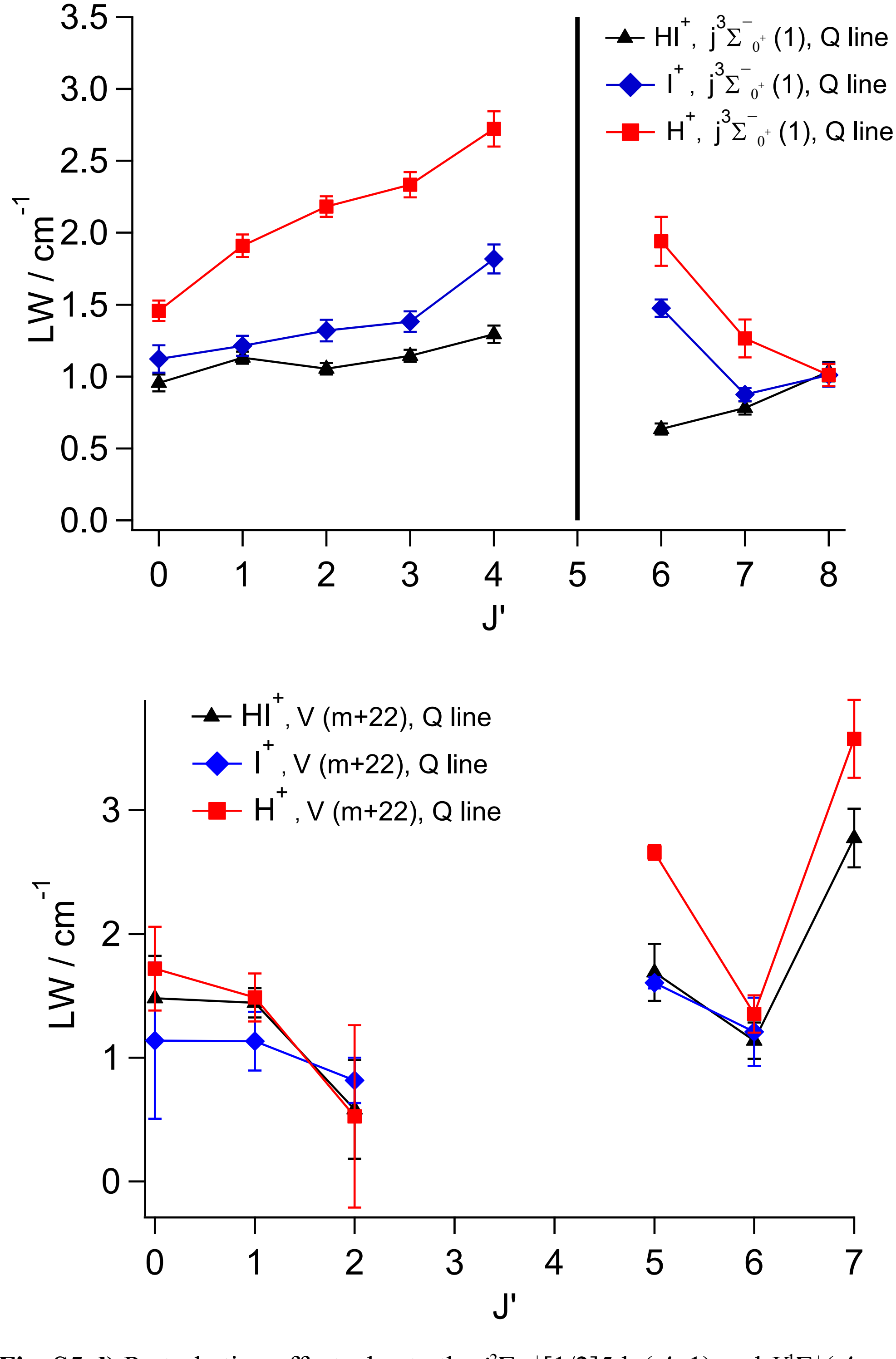


**Fig. S5 d)** Perturbation effects due to the $j^3\Sigma^-{}_0{}^+[1/2]5d\pi(v'=1)$ and $V^1\Sigma^+(v'=m+22)$ state interaction. Rotational line widths vs $J'$ derived from the $Q$ lines of ion-spectra for the $j^3\Sigma^-{}_0{}^+[1/2]5d\pi(v'=1)$ and $V^1\Sigma^+(v'=m+22)$ state spectra.

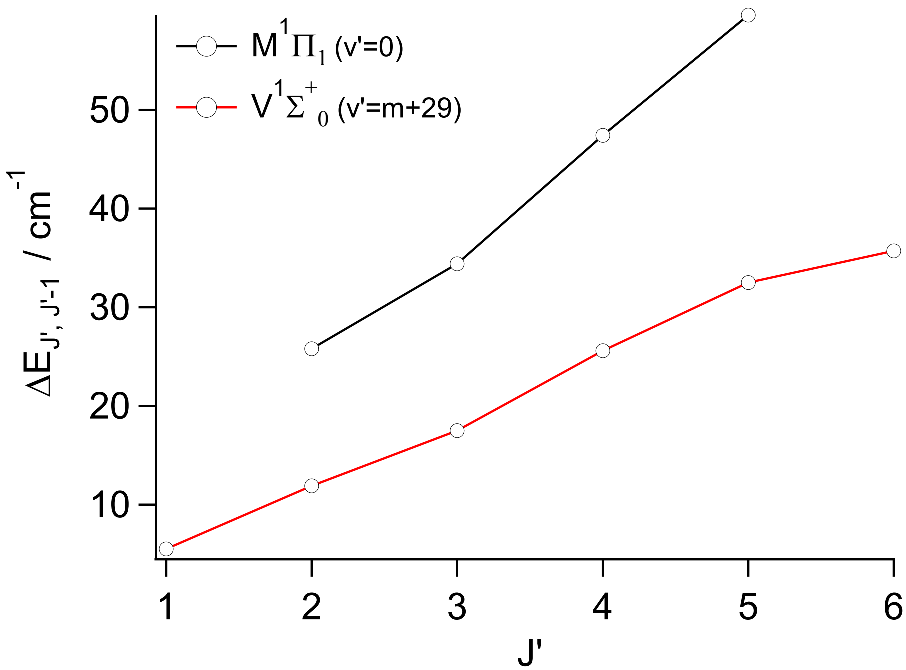


**Fig. S6 a)** Perturbation effects due to the $M^1\Pi_1$ [1/2]7s$\sigma$($v'$=0) and $V^1\Sigma^+$($v'$=$m$+29) states interaction. Spacing between rotational levels ($\Delta E_{J,\,J\text{-}1}$) as a function of $J'$.

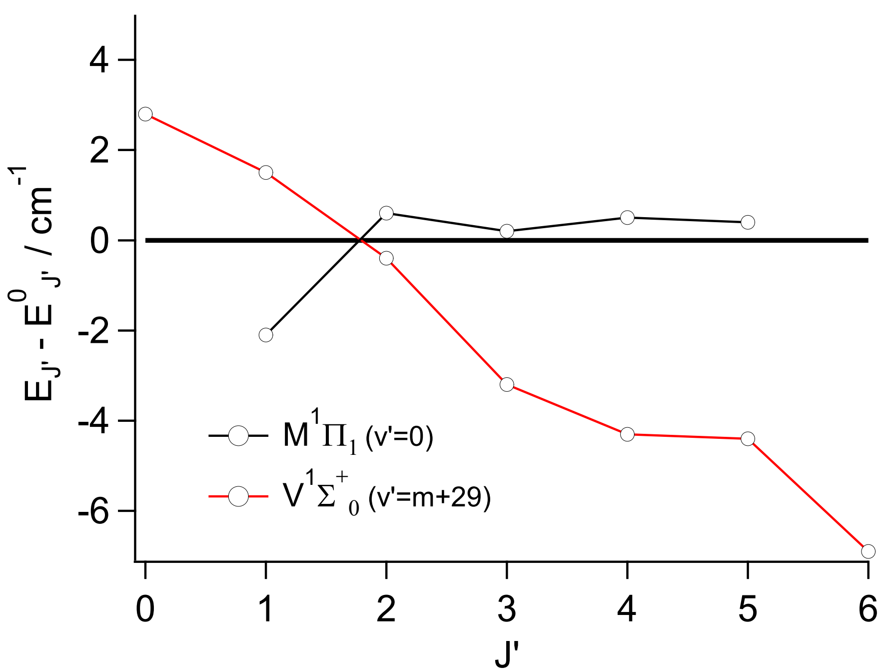


**Fig. S6 b)** Perturbation effects due to the $M^1\Pi_1$ [1/2]7s$\sigma$($v'$=0) and $V^1\Sigma^+$($v'$=$m$+29) states interaction. Reduced term value plots: Deperturbed energy level values subtracted from experimental energy level values.

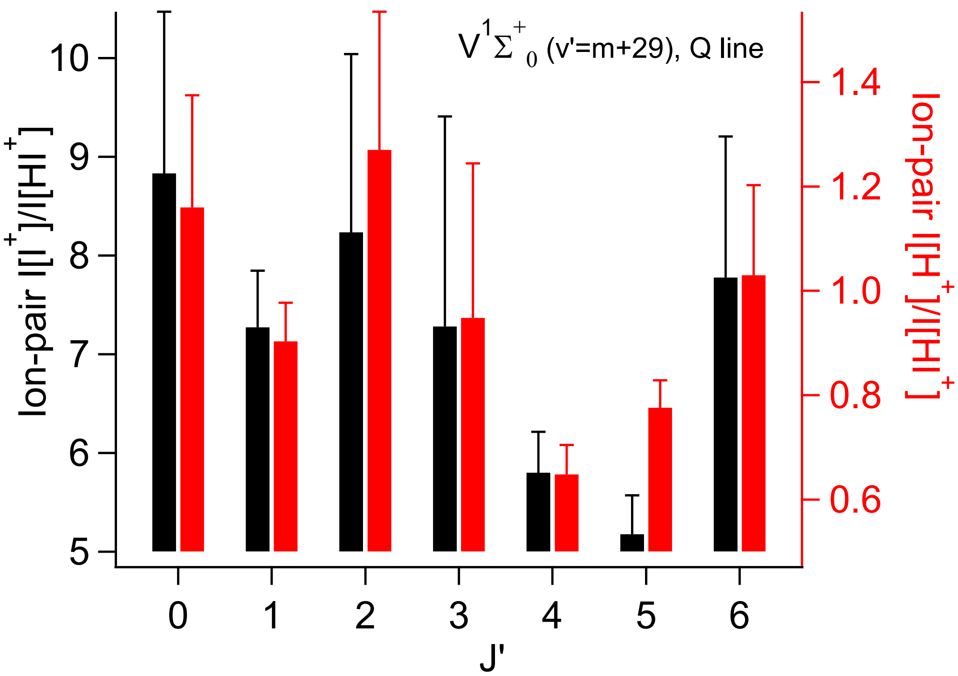


**Fig. S6 c)** Perturbation effects due to the $M^1\Pi_1$ [1/2]7s$\sigma$($v'$=0) and $V^1\Sigma^+$($v'$=$m$+29) states interaction. Relative ion-signal intensities ($I$($I^+$)/$I$($HI^+$) and $I$($H^+$)/$I$($HI^+$) vs. $J'$ derived from the $Q$-rotational lines for the $V^1\Sigma^+$($v'$=$m$+29) spectrum.

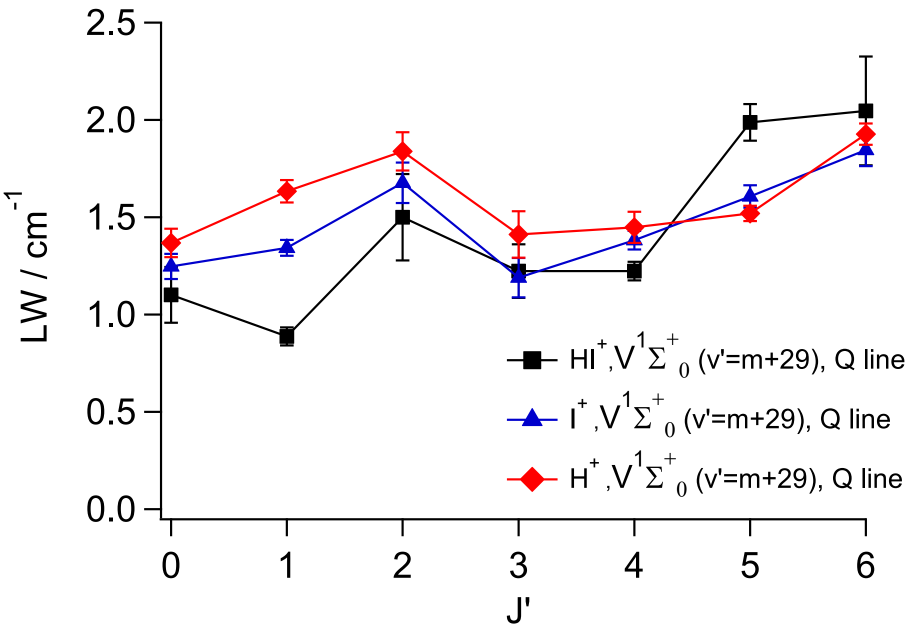


**Fig. S6 d)** Perturbation effects due to the $M^1\Pi_1$ [1/2]7s$\sigma$($v'$=0) and $V^1\Sigma^+$($v'$=$m$+29) states interaction. Rotational line-widths vs $J'$ derived from the $Q$ lines of the ion-spectra for the $V^1\Sigma^+$($v'$=$m$+29) state.

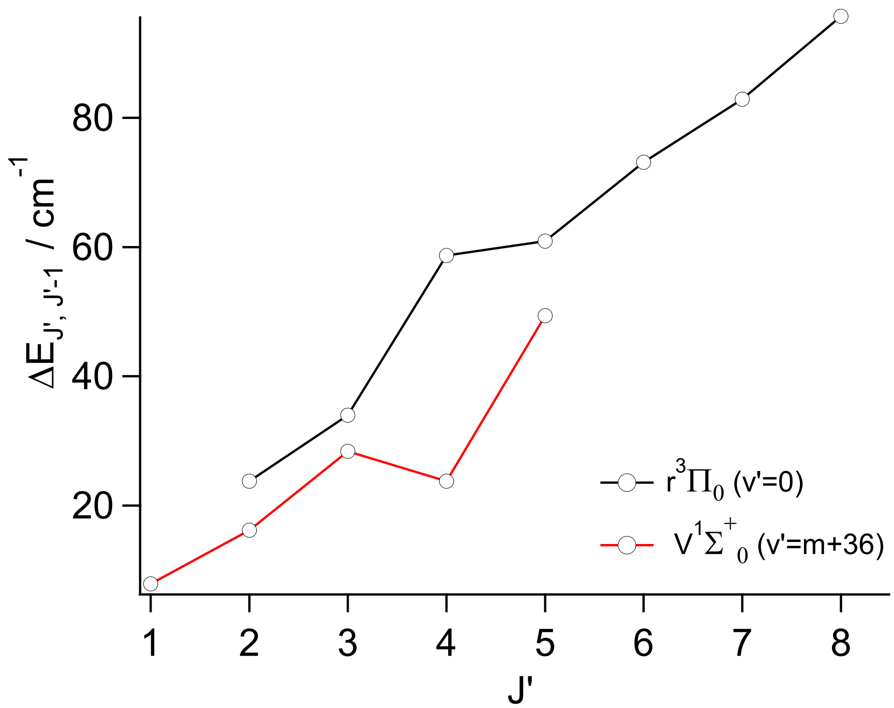


**Fig. S7 a)** Perturbation effects due to the $r^3\Pi_0$ [1/2]7p$\sigma$($v'$=0) and $V^1\Sigma^+$($v'$=$m$+36) state interaction. Spacing between rotational levels ($\Delta E_{J, J-1}$) as a function of $J'$.

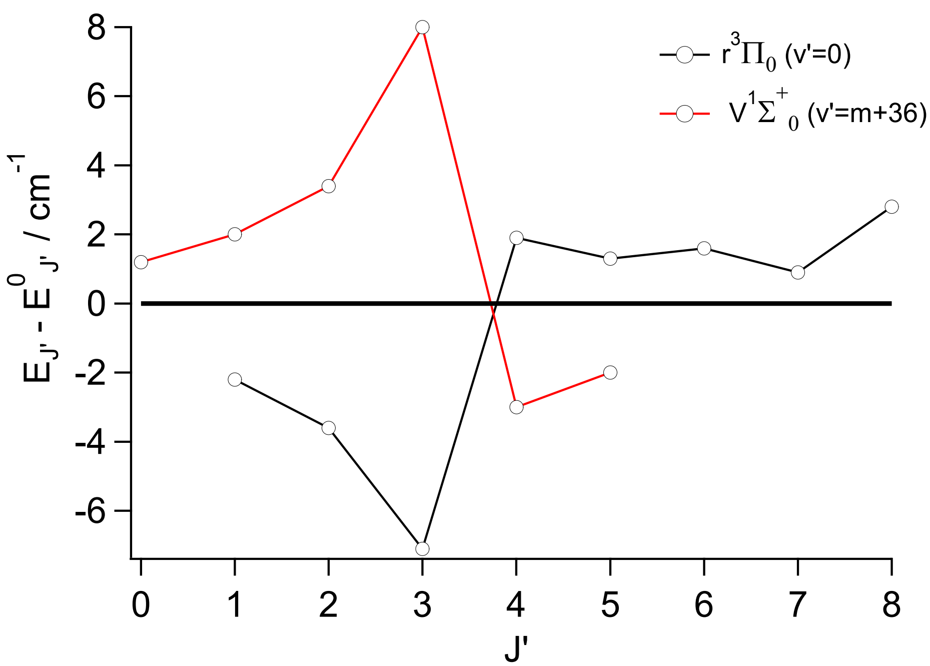


**Fig. S7 b)** Perturbation effects due to the $r^3\Pi_0$ [1/2]7p$\sigma$($v'$=0) and $V^1\Sigma^+$($v'$=$m$+36) state interaction. Reduced term value plots: Deperturbed energy level values subtracted from experimental energy level values.

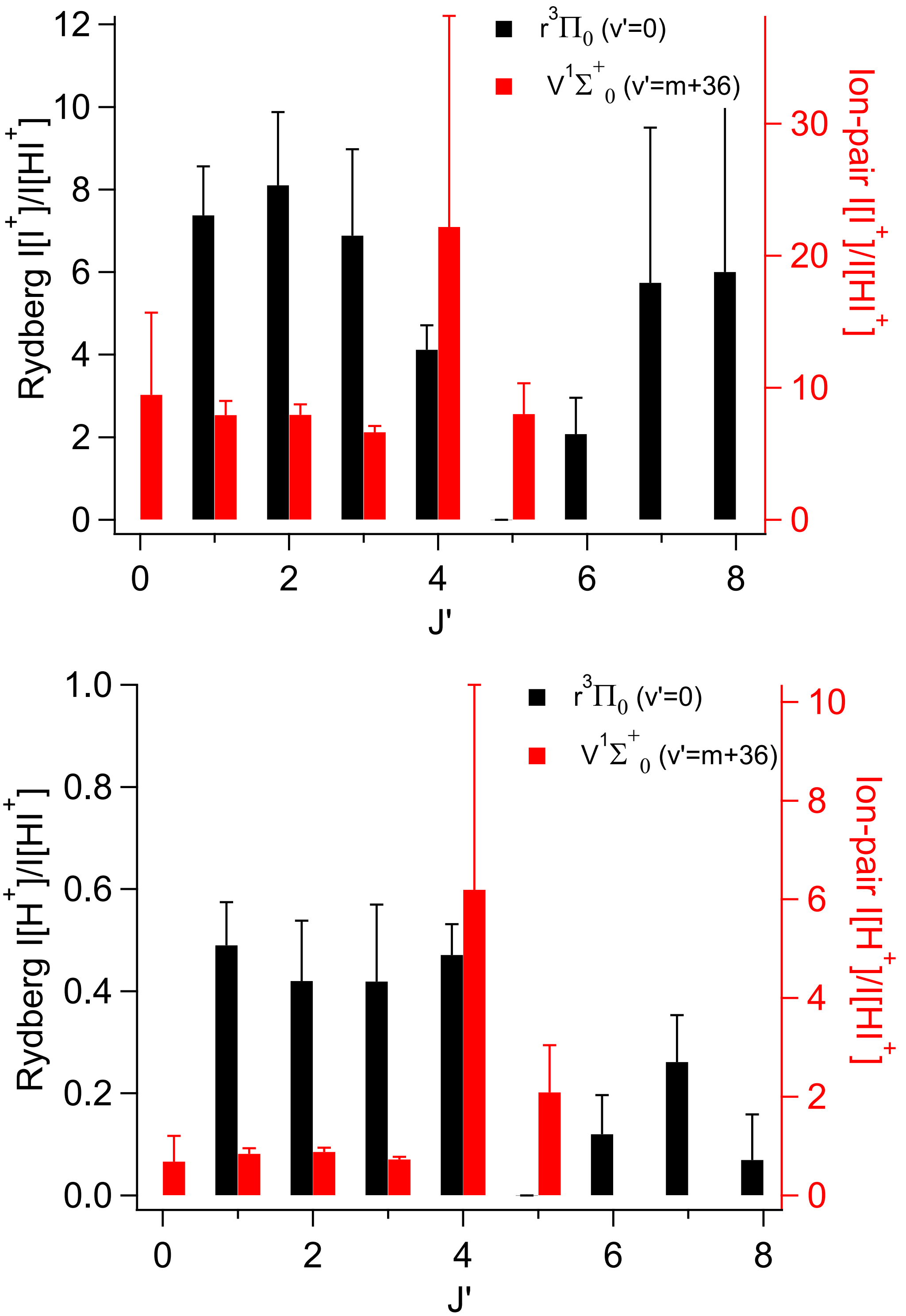


**Fig. S7 c)** Perturbation effects due to the $r^3\Pi_0$ [1/2]7p$\sigma$($v'$=0) and $V^1\Sigma^+$($v'$=$m$+36) state interaction. Relative ion-signal intensities ($I(I^+)/I(HI^+)$ and $I(H^+)/I(HI^+)$) vs. $J'$ derived from the $Q$-rotational lines for the $r^3\Pi_0$ [1/2]7p$\sigma$($v'$=0) and $V^1\Sigma^+$($v'$=$m$+36) spectra.

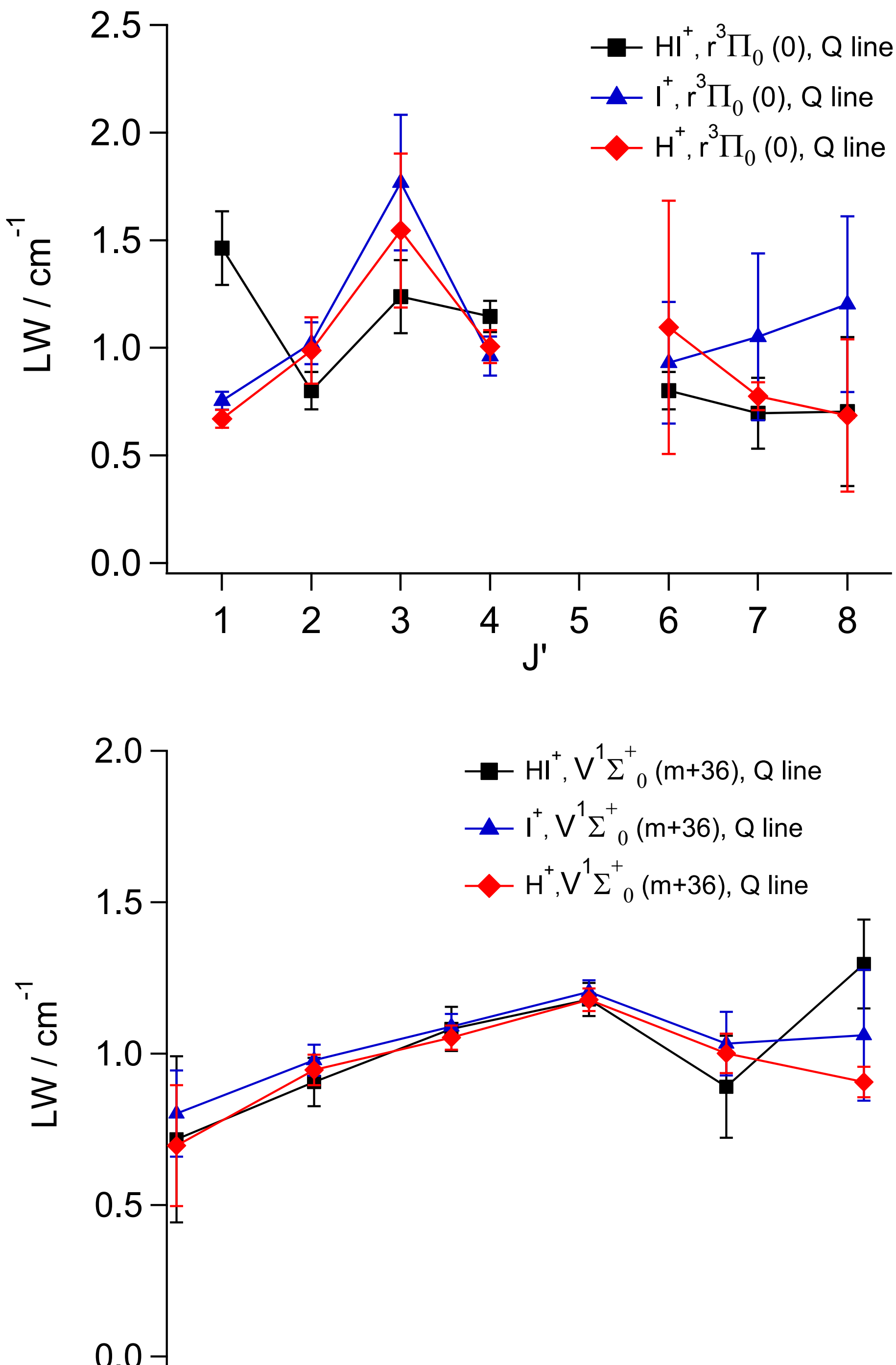


**Fig. S7 d)** Perturbation effects due to the $r^3\Pi_0$ [1/2]7p$\sigma$($v'$=0) and $V^1\Sigma^+$($v'$=$m$+36) state interaction. Rotational line widths vs. $J'$ derived from the $Q$ lines of the ion-spectra for the $r^3\Pi_0$ [1/2]7p$\sigma$($v'$=0) and $V^1\Sigma^+$($v'$=$m$+36) states.

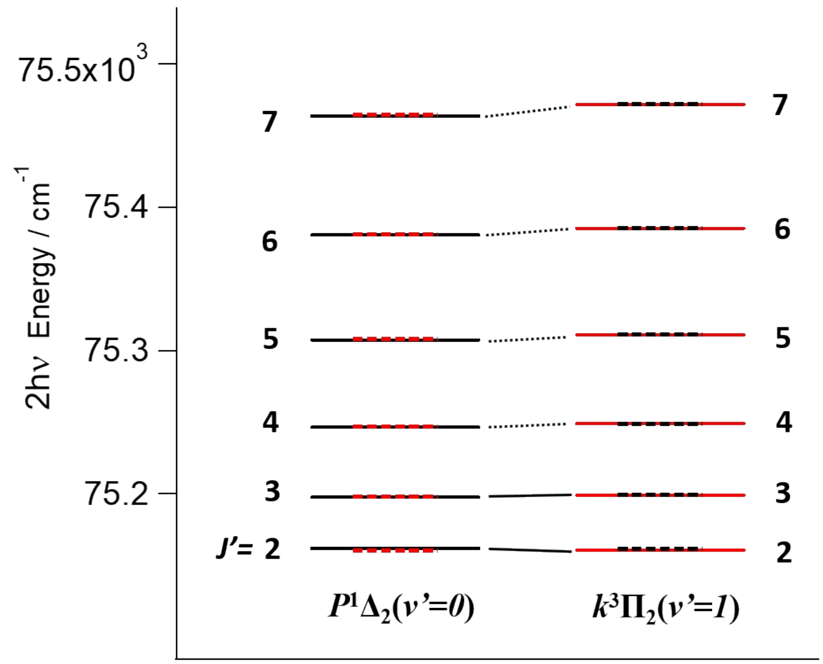


**Fig. S8 a)** Energy level diagram showing deperturbed (broken lines) and perturbed (solid lines) rotational energy levels for $P^1\Delta_2$ [1/2]4f$\pi$($v'$=0) and $k^3\Pi_2$ [1/2]5d$\delta$($v'$=1).

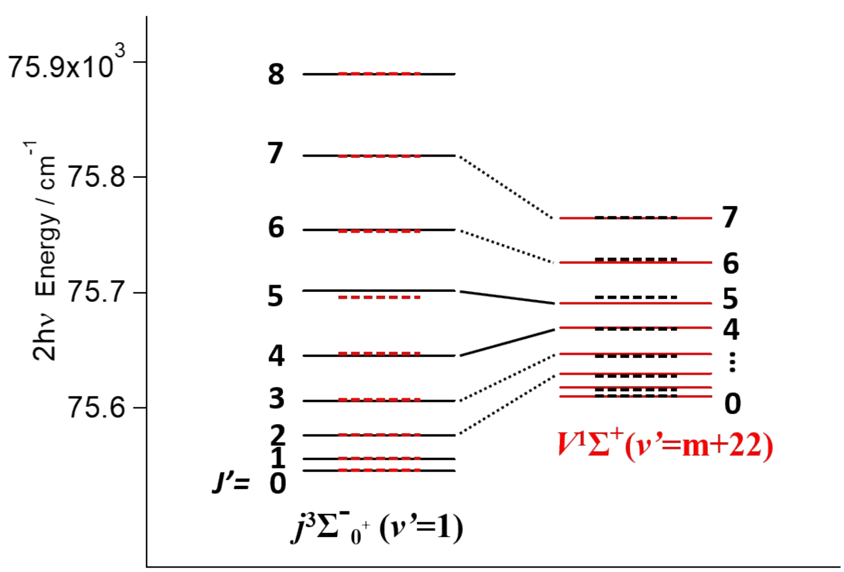


**Fig. S8 b)** Energy level diagram showing deperturbed (broken lines) and perturbed (solid lines) rotational energy levels for $j^3\Sigma^-_{0}{}^+$[1/2]5d$\pi$($v'$=1) and $V^1\Sigma^+$($v'$=$m$+22).

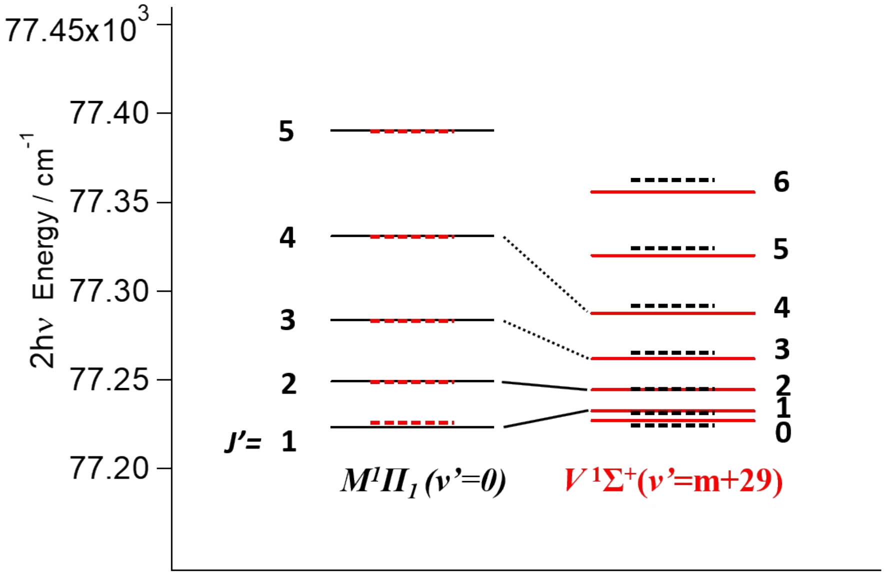


**Fig. S8 c)** Energy level diagram showing deperturbed (broken lines) and perturbed (solid lines) rotational energy levels for $M^1\Pi_1$ [1/2]7s$\sigma$($v'$=0) and $V^1\Sigma^+$($v'$=$m$+29).

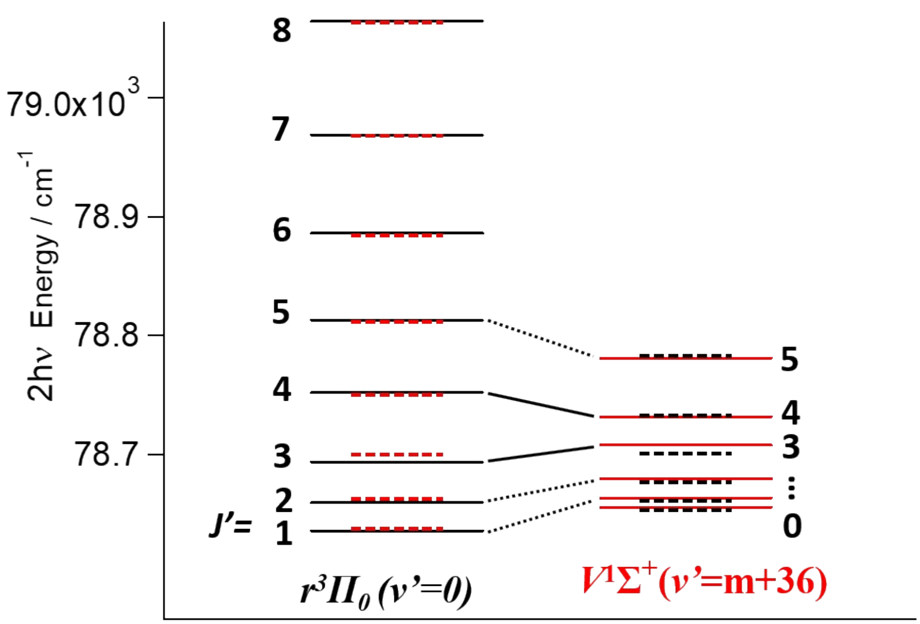


**Fig. S8 d)** Energy level diagram showing deperturbed (broken lines) and perturbed (solid lines) rotational energy levels for $r^1\Pi_0$ [1/2]7p$\sigma$($v'$=0) and $V^1\Sigma^+$($v'$=$m$+36).

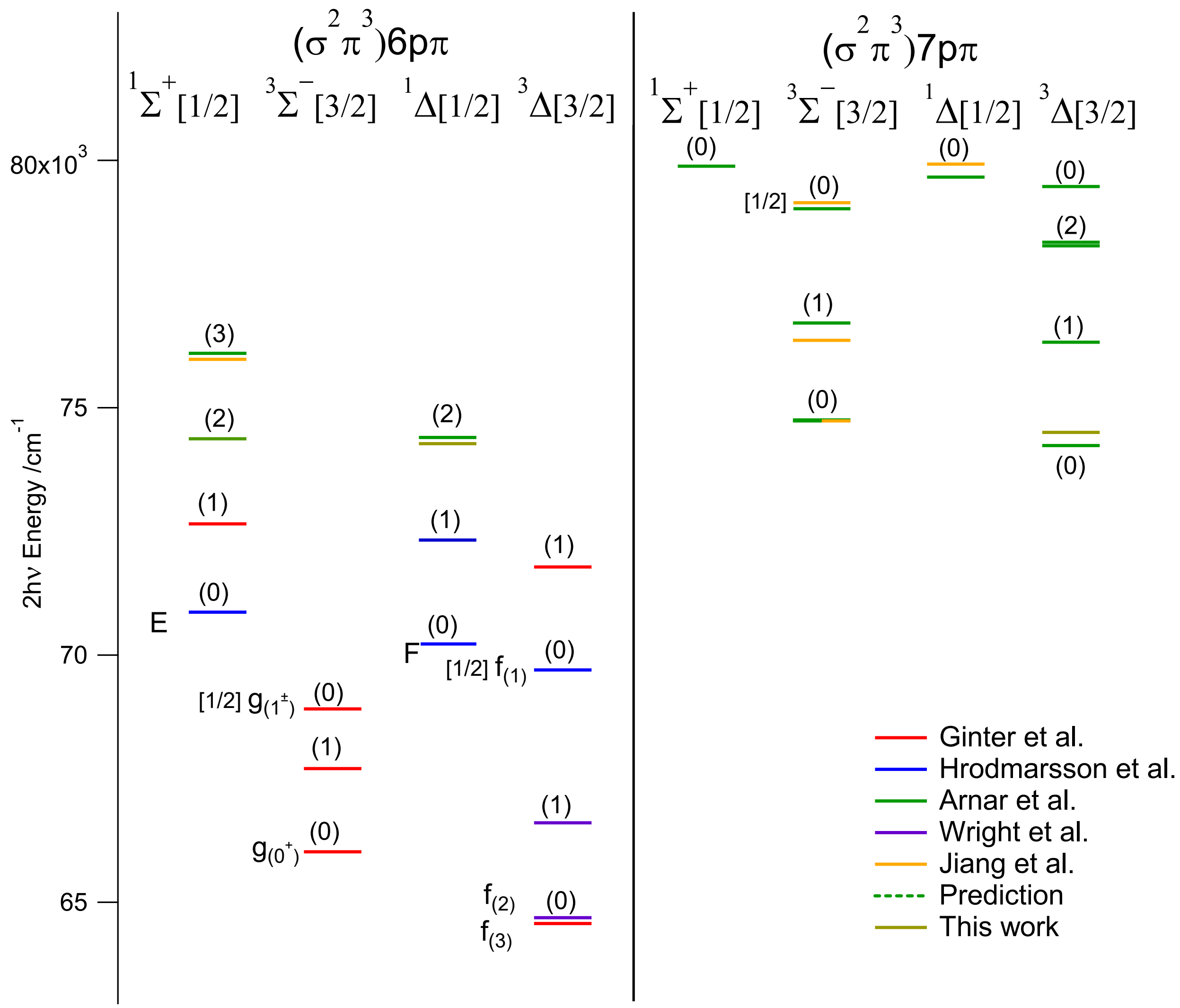


**Fig. S9 a)** $^{1,3}\Sigma$ and $^{1,3}\Delta$, $[\Omega_c]np\pi$ ($n$ = 6, 7) Rydberg states of HI.

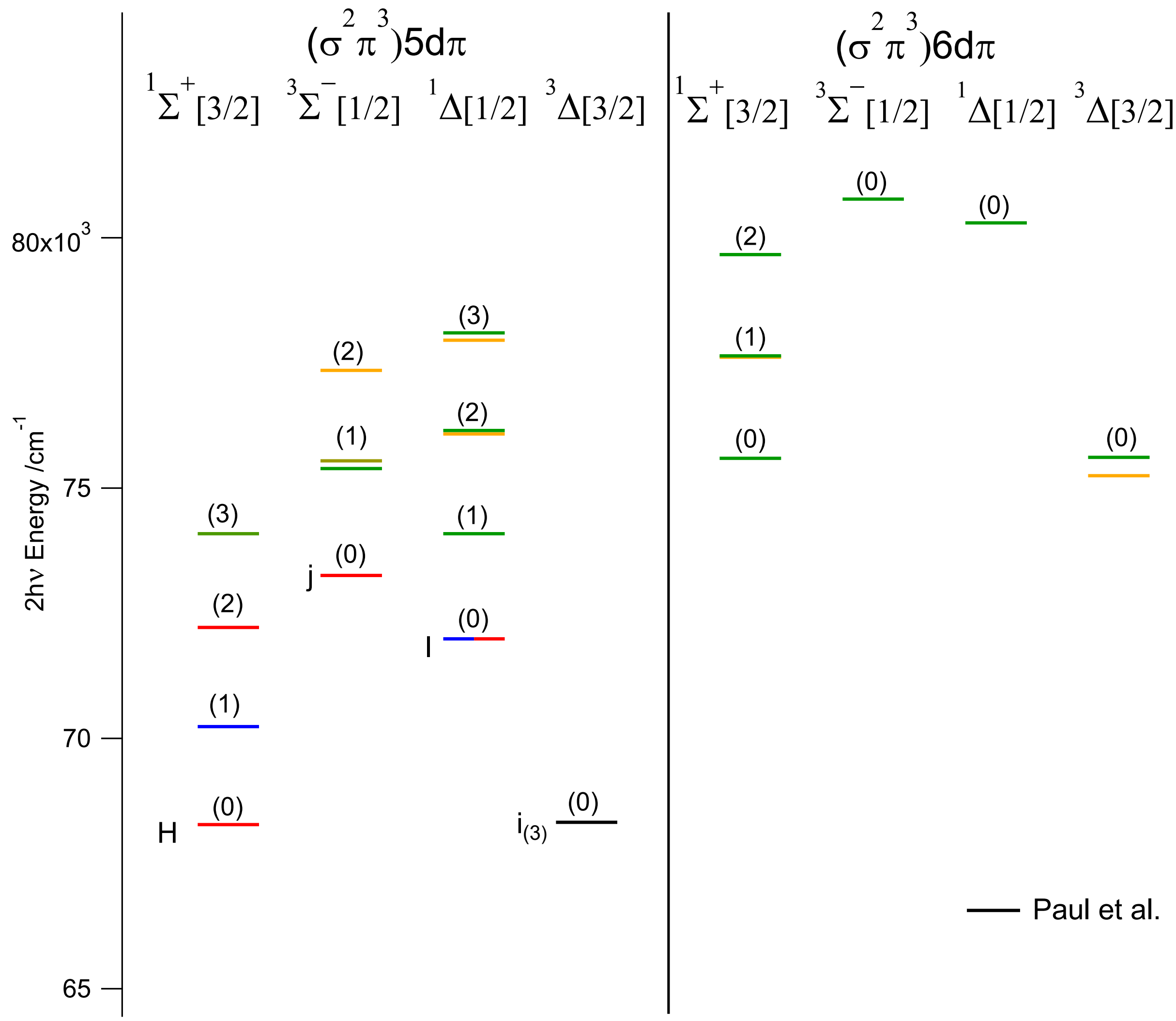


**Fig. S9 b)** $^{1,3}\Sigma$ and $^{1,3}\Delta$, $[\Omega_c]nd\pi$ ($n$ = 5, 6) Rydberg states of HI.

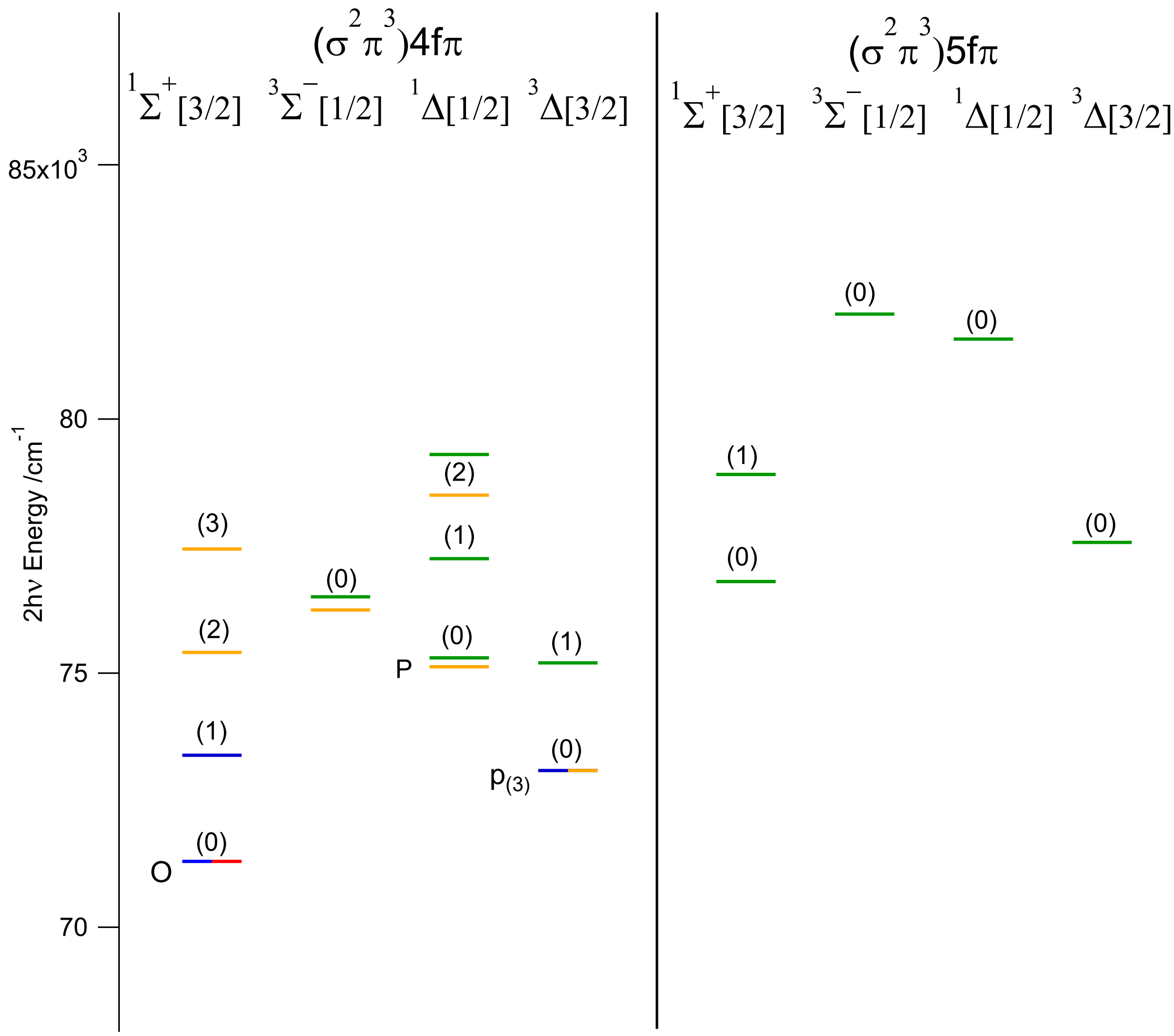


**Fig. S9 c)** $^{1,3}\Sigma$ and $^{1,3}\Delta$, $[\Omega_c]nf\pi$ ($n$ = 4, 5) Rydberg states of HI.

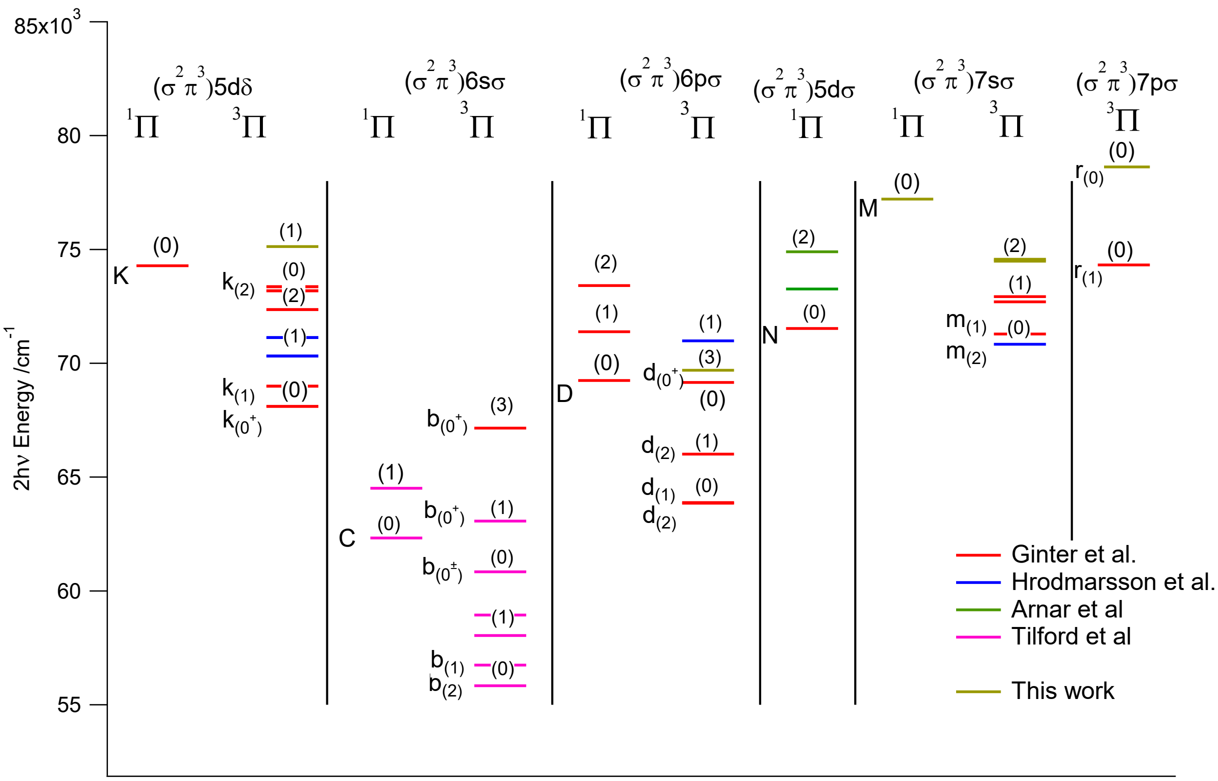


**Fig. S9 d)** $^{1,3}\Pi$ Rydberg states of HI with σ and δ Rydberg electrons.

**Fig. S9:** Energy level diagram of known Rydberg states for HI converging to the ground ionic states $X^2\Pi$ [3/2,1/2] as well as some predicted states.

a) $^{1,3}\Sigma$ and $^{1,3}\Delta$, $[\Omega_c]np\pi$ $(n = 6, 7)$ Rydberg states.

b) $^{1,3}\Sigma$ and $^{1,3}\Delta$, $[\Omega_c]nd\pi$ $(n = 5, 6)$ Rydberg states.

c) $^{1,3}\Sigma$ and $^{1,3}\Delta$, $[\Omega_c]nf\pi$ $(n = 4, 5)$ Rydberg states.

d) $^{1,3}\Pi$ Rydberg states with σ and δ Rydberg electrons.

Solid lines (different colors) correspond to previously detected bands [1-11] and present work (orange lines), as specified in the figures. Green dotted lines correspond to predicted states according to quantum defect analyses.

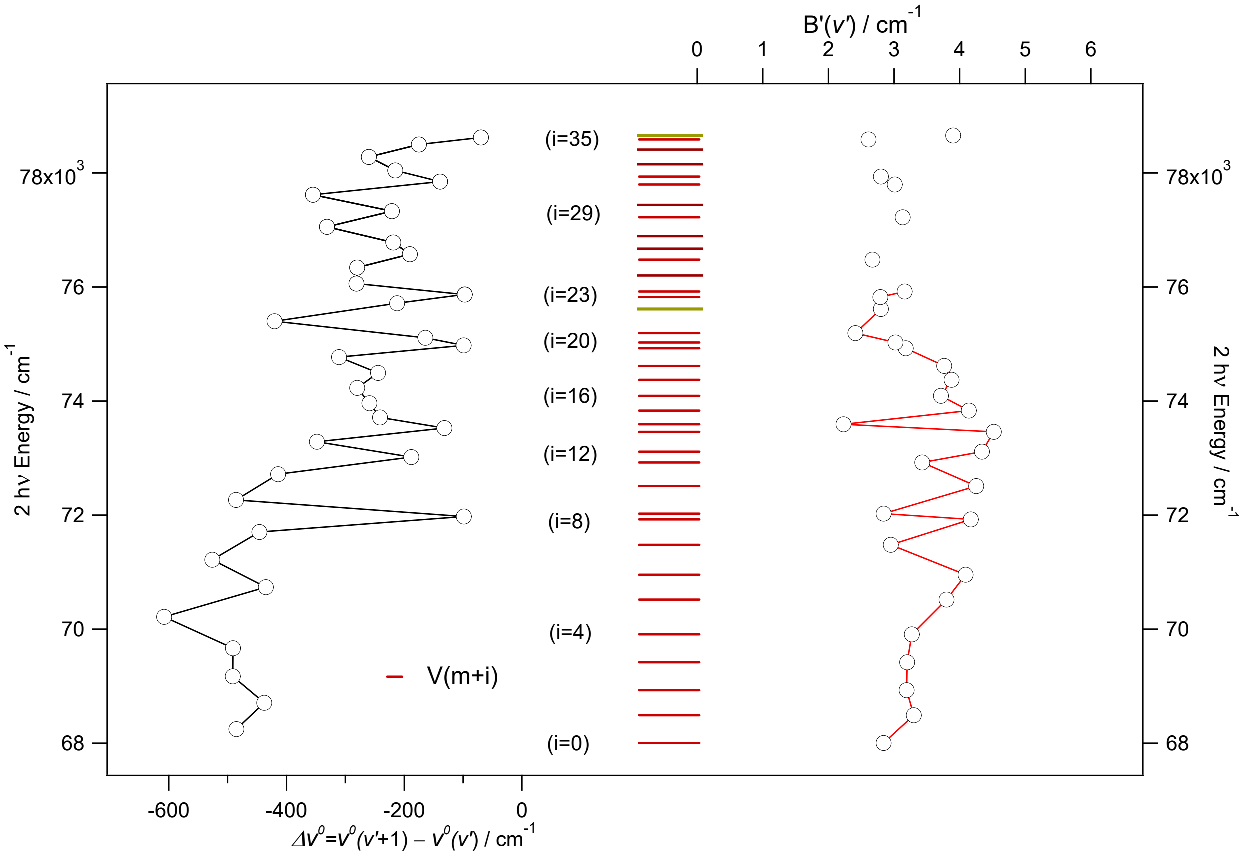


**Fig. S10** Vibrational energy levels the $V\ ^1\Sigma^+_{0+}(\sigma\pi^4)\sigma^*$ (red) ion-pair state as well as vibrational energy level spacing ($\Delta\nu^0(v' + 1, v') = \nu^0(v' + 1, v') - \nu^0(v')$) for the $V^1\Sigma^+$ ion-pair state (black curve rotated to the left) and rotational constants ($B'(v')$) (rotated to the right) (● – observed, ○–predicted or guessed.

# Tables:

## Table S1. Rotational lines of Rydberg and ion-pair state spectra:

**(a – c)**: Rotational lines for new Rydberg state spectra, (a) $d^3\Pi_1$[3/2] 6p$\sigma$($v'$=3), (b) $f^3\Delta_2$ [3/2]7p$\pi$ ($v'$=2) *and* (c) $m^3\Pi_{2,1}$[3/2]7s$\sigma$($v'$=2).

**(d – g)**: Rotational lines of Rydberg and ion-pair state spectra which exhibit state interactions, (d) $P^1\Delta_2$ [1/2]4f$\pi$($v'$=0) and $k^3\Pi_2$ [1/2]5d$\delta$($v'$=1), (e) $j^3\Sigma^-_0{}^+$[1/2]5d$\pi$($v'$=1) and $V^1\Sigma^+$($v'$=$m$+22), (f) $M^1\Pi_1$ [1/2]7s$\sigma$($v'$=*0*) and $V^1\Sigma^+$($v'$=$m$+29) (g) $r^1\Pi_1$ [1/2]7p$\sigma$($v'$=0) and $V^1\Sigma^+$($v'$=$m$+36)

.

***Table S1a.*** Rotational line wavenumbers for the HI $d^3\Pi_1$ [3/2]6p$\sigma$←← $X\,^1\Sigma^+$ (3,0) spectrum.

| J' | O (J) | P (J) | Q (J) | R (J) | S (J) |
|---|---|---|---|---|---|
| 0 | | | | | |
| 1 | 69624.5 | 69662.5 | 69691.1 | 69714.5 | |
| 2 | 69597.9 | 69647.5 | 69689.9 | 69724.3 | 69729.5 |
| 3 | 69572.7 | 69631.6 | | 69733.6 | 69752.9 |
| 4 | 69546.2 | 69614.7 | | 69741.0 | 69775.2 |
| 5 | 69516.6 | | | 69747.4 | 69796.1 |
| 6 | | | | | 69818.1 |
| 7 | | | | | 69839.6 |
| 8 | | | | | |

***Table S1b.*** Rotational line wavenumbers for the HI $f^3\Delta_2$ [3/2]7p$\pi$←← $X\,^1\Sigma^+$ (0,0) spectrum.

| J' | O (J) | P (J) | Q (J) | R (J) | S (J) |
|---|---|---|---|---|---|
| 0 | | | | | |
| 1 | | | | | |
| 2 | 74406 | 74471.7 | 74494.1 | 74530.8 | 74534.0 |
| 3 | | 74455.2 | 74491.3 | 74539.2 | 74555.2 |
| 4 | | 74438.0 | 74484.9 | 74547.2 | 74575.2 |
| 5 | | 74420.8 | 74477.7 | 74555.2 | 74593.7 |
| 6 | | 74409.6 | 74469.3 | 74562.4 | 74627.8 |
| 7 | | | 74452.8 | 74568.8 | 75282.1 |
| 8 | | | | | |

***Table S1c.*** Rotational line wavenumbers for the HI $m^3\Pi_{2,1}[3/2]7s\sigma \leftarrow\leftarrow X\,^1\Sigma^+$ (2,0) spectrum.

| ***J′*** | ***O* (*J*)** | ***P* (*J*)** | ***Q* (*J*)** | ***R* (*J*)** | ***S* (*J*)** |
|---|---|---|---|---|---|
| | | | $m^3\Pi_2$ | | |
| 0 | | | | | |
| 1 | | | | | |
| 2 | | 74463.3 | | 74501.3 | |
| 3 | | 74446.4 | | 74507.4 | |
| 4 | | 74428.4 | | 74510.9 | |
| 5 | | | | 74514.2 | |
| 6 | | | | 74518.2 | |
| 7 | | | | 74522.2 | |
| 8 | | | | 74526.4 | |
| | | | $m^3\Pi_1$ | | |
| 0 | | | | | |
| 1 | 74507.4 | 74555.2 | 74570.0 | 74604.1 | |
| 2 | | | | | 74606.5 |

***Table S1d.*** Rotational line wavenumbers for the HI $P^1\Delta_2$ [1/2]4f$\pi$($v'$=0) and $k^3\Pi_2$ [1/2]5d$\delta$($v'=1$)$\leftarrow\leftarrow X\,^1\Sigma^+$ ($v''=0$) spectra.

| ***J′*** | ***O* (*J*)** | ***P* (*J*)** | ***Q* (*J*)** | ***R* (*J*)** | ***S* (*J*)** |
|---|---|---|---|---|---|
| | | | $P^1\Delta_2$ | | |
| 0 | | | | | |
| 1 | | | | | |
| 2 | 75033.8 | 75086.3 | 75123.8 | 75147.6 | 75159.9 |
| 3 | 75005.8 | 75072.5 | 75121.4 | 75159.8 | 75180.8 |
| 4 | | 75058.1 | 75119.6 | 75169.9 | 75208.4 |
| 5 | | 75042.9 | 75117.4 | 75181.0 | 75232.6 |
| 6 | | 75026.8 | 75114.6 | 75191.3 | 75257.6 |
| 7 | | 75011 | 75109.4 | | 75282.1 |
| | | | $k^3\Pi_2$ | | |
| 0 | | | | | |
| 1 | | | | | |
| 2 | 75059.9 | | 75122.4 | | 75158.7 |
| 3 | | | 75123.0 | | 75184.1 |
| 4 | | | 75122.1 | | |
| 5 | | | 75120.9 | | |
| 6 | | | 75119.4 | | |
| 7 | | | 75117.5 | | |

***Table S1e.*** Rotational line wavenumbers for the HI $j^3\Sigma^-_0{}^+$[1/2]5d$\pi$($v'$=1) and $V^1\Sigma^+$($v'$=$m$+22)←← X $^1\Sigma^+$ ($v''$=0) spectra.

| ***J'*** | ***Q (J)*** | ***Q (J)*** |
|---|---|---|
| | $j^3\Sigma^-_0{}^+$ | $V^1\Sigma^+$ |
| 0 | 75545.5 | 75610.0 |
| 1 | 75543.1 | 75604.8 |
| 2 | 75538.3 | 75591.7 |
| 3 | 75530.2 | 75570.5 |
| 4 | 75518.6 | 75542.5 |
| 5 | 75511.4 | 75500.4 |
| 6 | 75488.5 | 75460.1 |
| 7 | 75464.1 | 75410.1 |
| 8 | 75434.0 | |

***Table S1f.*** Rotational line wavenumbers for the HI $M^1\Pi_1$ [1/2]7s$\sigma$($v'$=0) and $V^1\Sigma^+$($v'$=$m$+29)←← X $^1\Sigma^+$ ($v''$=0) spectra.

| ***J'*** | ***O (J)*** | ***P (J)*** | ***Q (J)*** | ***R (J)*** | ***S (J)*** | ***Q (J)*** |
|---|---|---|---|---|---|---|
| | | | $M^1\Pi_1$ | | | $V^1\Sigma^+$ |
| 0 | | | | | | 77226.9 |
| 1 | 77149.2 | 77183.3 | 77210.64 | 77232.3 | | 77219.7 |
| 2 | | 77168.4 | 77211.09 | 77241.1 | 77245.8 | 77206.2 |
| 3 | | 77152.2 | 77207.46 | 77249.3 | 77270.6 | 77185.7 |
| 4 | | 77134.6 | 77204.14 | 77255.1 | 77296.2 | 77160.6 |
| 5 | | | 77200.43 | | | 77129.8 |
| 6 | | | | | | 77089.6 |
| 7 | | | | | | |
| 8 | | | | | | |

***Table S1g.*** Rotational line wavenumbers for the HI $r^3\Pi_0$ [1/2]7p$\sigma$($v'$=0) and $V^1\Sigma^+$($v'$=$m$+36) ←← $X\,^1\Sigma^+$ ($v''$=0) spectra.

| ***J′*** | ***Q (J)*** | ***Q (J)*** |
|---|---|---|
| | $r^3\Pi_0$ | $V^1\Sigma^+$ |
| 0 | | 78655.2 |
| 1 | 78622.8 | 78650.4 |
| 2 | 78621.2 | 78641.2 |
| 3 | 78617.2 | 78631.6 |
| 4 | 78625.2 | 78604.7 |
| 5 | 78622.8 | 78590.8 |
| 6 | 78620.0 | |
| 7 | 78614.4 | |
| 8 | 78609.1 | |

## Table S2.

a) **New HI Rydberg states:** Rydberg state specifications ($Ry\ ^{2S+1}\Lambda_\Omega[\Omega_c]nl\lambda$) (see main text), vibrational quantum numbers (***v′***), symmetry, band origin (**ν⁰**), rotational parameters (***B′***,***D′***), relative intensities, quantum defect values (***δ***) and line series observed in Rydberg state spectra.

| State specifications | v' | Symmetry | $\nu^0$ /cm$^{-1}$ | *B′*/ cm$^{-1}$ | *D′**10$^4$ / cm$^{-1}$ | Int. | Quantum defect *δ* | Line series observed |
|---|---|---|---|---|---|---|---|---|
| $d^3\Pi_1$[3/2] 6p$\sigma$ | 3 | e | 69691.6 | 6.08 | 3.7 | vw | 3.67 | *O,Q,S* |
| | | f | 69691.6 | 5.93 | 18.0 | | | *P,R* |
| $f^3\Delta_2$ [3/2]7pπ | 0 | e | 74500.9 | 5.58 | -8.4 | w | 3.56 | *O,Q,S* |
| | | f | 74509.4 | 5.69 | 35.8 | | | *P,R* |
| $m^3\Pi_2$[1/2]7s$\sigma$ | 2 | f | 74484.1 | 5.10 | -57.8 | w | 4.14 | *P,R* |
| $m^3\Pi_1$[1/2]7s$\sigma$ | 2 | e | 74571.3 | 5.90 | --- | w | 4.13 | *O,Q,S* |
| | | f | 74581.8 | 5.81 | | | | *P,R* |

**b) Interacting Rydberg and ion-pair states:** Rydberg and ion-pair states specifications (*Ry* $^{2S+1}\Lambda_{\Omega}[\Omega_c]nl\lambda$) (see main text), vibrational quantum numbers (***v'***), symmetry, band origin (**v⁰**), rotational parameters (***B'***,***D'***), relative intensities, quantum defect values (***δ***) and line series observed in Rydberg state spectra.

| State specifications | v' | Symm. | $v^0$ /cm$^{-1}$ | B'/ cm$^{-1}$ | D'*10$^4$ / cm$^{-1}$ | Int. | Quantum defect δ | Line series observed |
|---|---|---|---|---|---|---|---|---|
| $P^1\Delta_2$ [1/2]4f$\pi$ | 0 | e | 75124.9 [a] | 6.11 [a] | 9.8 [a] | ms | 1.20 | *O,Q,S* |
| | | | 75123.0 [b] | 6.27 [b] | 30.9 [b] | | | |
| | | f | 75124.6 [a] | 6.15 [a] | 7.8 [a] | | | *P,R* |
| $k^3\Pi_2$ [1/2]5d$\delta$ | 1 | e | 75123.0 [a] | 6.26 [a] | 7.9 [a] 7.0[b] | ms | 2.39 | *Q,S* |
| | | | 75124.0[b] | 6.26[b] | | | | |
| | | | | | | | | |
| $j^3\Sigma^-_0{}^+$[1/2]5d$\pi$ | 1 | e | 75546.1 [a] | 5.14 [a] | 54.0 [a] | vs | 2.36 | *Q* |
| | | | 75546.0 [b] | 5.16 [b] | 54.8 [b] | | | |
| $V^1\Sigma^+$ | *m*+22 | e | 75612.6 [a] | 2.80 [a] | 12.0 [a] | m | | |
| | | | 75610.0 [b] | 2.98 [b] | 38.8 [b] | | | |
| | | | | | | | | |
| $M^1\Pi_1$ [1/2]7s$\sigma$ | 0 | e | 77212.1 [a] | 5.97 [a] | -81.0 [a] | vw | 3.96 | *O,Q,S* |
| | | | 77214.0 [b] | 5.72 [b] | -50.6 [b] | | | |
| | | f | 77211.9 [a] | 5.87 [a] | -20.0 [a] | | | *P,R* |
| $V^1\Sigma^+$ | *m*+29 | e | 77226.8 [a] | 2.98 [a] | -26.0 [a] | m | | *Q* |
| | | | 77224.0 [b] | 3.46 [b] | 38.4 [b] | | | |
| | | | | | | | | |
| $r^3\Pi_0$ [1/2]7p$\sigma$ | 0 | e | 78623.0 [a] | 6.30 [a] | 28.0 [a] | s | 3.76 | *Q* |
| | | | 78625.0 [b] | 6.33 [b] | 35.8 [b] | | | |
| $V^1\Sigma^+$ | *m*+36 | e | 78655.0 [a] | 3.90 [a] | -65.0 [a] | ms | | *Q* |
| | | | 78654.0 [b] | 3.48 [b] | -27.1 [b] | | | |
| | | | | | | | | |

[a]Underperturbed(perturbed) values; this work
[b] Derperturbed values; this work

**Table S3.** State interactions; $J'$ level proximity ($\Delta E_{J'} = E_{J'}(1) - E_{J'}(2)$ / cm$^{-1}$), interaction strength ($W_{12}$ / cm$^{-1}$) and fractional state mixing ($c_1^2$, $c_2^2$).

| $P^1\Delta_2$ [1/2]4f$\pi$($v'$ = 0) $\leftrightarrow$ $k^3\Pi_2$ [1/2]5d$\delta$($v'$ = 1) | | | | |
|---|---|---|---|---|
| $J'$ | $\Delta E_{J'}$ | $W_{12}$ | $c_1^2$ | $c_2^2$ |
| 2 | -1.4 | 0.7 | 0.647 | 0.353 |
| 3 | 1.6 | 0.7 | 0.753 | 0.247 |
| 4 | 2.5 | 0.7 | 0.917 | 0.083 |
| 5 | 3.5 | 0.7 | 0.960 | 0.040 |
| 6 | 4.8 | 0.7 | 0.979 | 0.021 |
| 7 | 8.1 | 0.7 | 0.993 | 0.007 |

| $j^3\Sigma^-{}_{0^+}$[1/2]5d$\pi$($v'$=1) $\leftrightarrow$ $V^1\Sigma^+$($v'$ = $m$ + 22) | | | | |
|---|---|---|---|---|
| $J'$ | $\Delta E_{J'}$ | $W_{12}$ | $c_1^2$ | $c_2^2$ |
| 0 | 64.5 | 6.4 | 0.990 | 0.010 |
| 1 | 61.7 | 6.4 | 0.989 | 0.011 |
| 2 | 53.4 | 6.4 | 0.986 | 0.014 |
| 3 | 40.3 | 6.4 | 0.974 | 0.026 |
| 4 | 23.9 | 6.4 | 0.923 | 0.077 |
| 5 | -12.8 | 6.4 | 0.438 | 0.562 |
| 6 | -28.4 | 6.4 | 0.947 | 0.053 |
| 7 | -54.0 | 6.4 | 0.986 | 0.014 |

| $M^1\Pi_1$ [1/2]7s$\sigma$($v'$=0) $\leftrightarrow$ $V^1\Sigma^+$($v'$ = $m$ + 29) | | | | |
|---|---|---|---|---|
| $J'$ | $\Delta E_{J'}$ | $W_{12}$ | $c_1^2$ | $c_2^2$ |
| 1 | 9.1 | 0.6 | 0.996 | 0.004 |
| 2 | -4.9 | 1.0 | 0.959 | 0.041 |
| 3 | -21.8 | 1.4 | 0.996 | 0.004 |
| 4 | -43.5 | 1.8 | 0.998 | 0.002 |
| 5 | -70.5 | 2.2 | 0.999 | 0.001 |

| $r^3\Pi_0$ [1/2]7p$\sigma$($v'$= 0) $\leftrightarrow$ $V^1\Sigma^+$($v'$= $m$ + 36) | | | | |
|---|---|---|---|---|
| $J'$ | $\Delta E_{J'}$ | $W_{12}$ | $c_1^2$ | $c_2^2$ |
| 1 | 27.6 | 7.2 | 0.927 | 0.073 |
| 2 | 20.0 | 7.2 | 0.848 | 0.152 |
| 3 | 14.4 | 7.2 | 0.531 | 0.469 |
| 4 | -20.5 | 7.2 | 0.857 | 0.143 |
| 5 | -40.1 | 7.2 | 0.967 | 0.033 |
| 6 | -59.9 | 7.2 | 0.985 | 0.015 |

**Table S4.** Summary of Rydberg states and spectra, previously observed and reassigned[a]. Rydberg state specifications ($Ry\ ^{2S+1}\Lambda_{\Omega}[\Omega_c]nl\lambda$), vibrational quantum numbers ($\boldsymbol{v'}$), band origin ($\mathbf{v^0}$), rotational parameters ($\boldsymbol{B'}$, $\boldsymbol{D'}$), quantum defect values ($\boldsymbol{\delta}$) and references of previous observations.

| **State specifications** | ***v'*** | **$v^0$ /cm$^{-1}$** | ***B'* / cm$^{-1}$** | ***D'**10$^4$ /cm$^{-1}$** | **Quantum defect *δ*** | **Refs.** |
|---|---|---|---|---|---|---|
| **$[\Omega_c]n$s$\sigma$ ($n$ = 6,7)** | | | | | | |
| $b\ ^3\Pi_2[3/2]6s\sigma$ | 0 | 55 833.1 | 6.348 | -- | 4.02 | [1] |
| | 1 | 58 040.5 | 6.173 | -- | 4.02 | [1] |
| $b\ ^3\Pi_1[3/2]6s\sigma$ | 0 | 56 738.3 | 6.427 | -- | 3.99 | [1] |
| | 1 | 58 937±20 | -- | -- | 3.98 | [1] |
| $b\ ^3\Pi_0^{\pm}[1/2]6s\sigma$ | 0 | 60 857.9 | 6.426 | -- | 4.03 | [1] |
| | 1 | 63 064.0 | 6.245 | -- | 4.03 | [1] |
| | 3 | 67 150.3 | 5.693 | 2.3 | 4.02 | [2] |
| $C\ ^1\Pi_1[1/2]6s\sigma$ | 0 | 62 325±10 | -- | -- | 3.97 | [1] |
| | 1 | 64 508±10 | -- | -- | 3.89 | [1] |
| $m\ ^3\Pi_2[3/2]7s\sigma$ | 0 | 70 837.6/70 841.5 | 6.11/ 6.21 ± 0.04 | 1.94/ 12± 5 | 4.09 | [3]/[4] |
| | 1 | 72 697.2 | 6.014 | 2.30 | 4.12 | [3] |
| | 2 | 74484.1 | 5.10 | -57.8 | 4.14 | [11] |
| $m\ ^3\Pi_1[3/2]7s\sigma$ | 0 | 71 287.3 | 6.254 | 3.18 | 4.04 | [3] |
| | 1 | 72 924.8/72 945.0 | 6.205/6.16 | 4.6/−16 | 4.09 | [3]/[6] |
| | 2 | 74571.3 | 5.90 | --- | 4.13 | [11] |
| $M^1\Pi_1\ [1/2]7s\sigma$ | 0 | 77212.1 | 5.97 | -81.0 | 3.96 | [11] |
| **$[\Omega_c]n$p$\sigma$ ($n$ = 6,7)** | | | | | | |
| $d\ ^3\Pi_2[3/2]6p\sigma$ | 0 | 63 854.9 | 6.065 | 1.7 | 3.65 | [2] |
| | 1 | 66 009.4 | 5.926 | 1.5 | 3.65 | [2] |
| $d\ ^3\Pi_1[3/2]6p\sigma$ | 0 | 63 883 | -- | -- | | [2] |
| | 3 | 69691.6 | 6.08 | 3.7 | 3.67 | [11] |
| $d\ ^3\Pi_0^+[1/2]6p\sigma$ | 0 | 69 157 | 6.117 | 2.1 | 3.65 | [2] |
| | 1 | 70 988.2 | 5.79 ± 0.12 | −290 ± 40 | 3.67 | [4] |
| $D^1\Pi_1[1/2]6p\sigma$ | 0 | 69 244.5 | 6.198 | 2.1 | 3.65 | [2]/[3] |
| | 1 | 71 382.4 | 6.052 | 1.92 | 3.65 | [3] |
| | 2 | 73 412.3 | 5.937 | 12.6 | 3.65 | [3] |

| | | | | | | |
|---|---|---|---|---|---|---|
| $r\ ^3\Pi_1[3/2]7p\sigma$ | 0 | 74 320 | 6.040 | -4.48 | 3.59 | [3] |
| $r^3\Pi_0\ [1/2]7p\sigma$ | 0 | 78623.0 | 6.30 | 28.0 | 3.76 | [11] |
| **[$\Omega_c$]*n*p$\pi$ *(n = 6,7)*** | | | | | | |
| $E\ ^1\Sigma^+[1/2]6p\pi$ | 0 | 70 850.5/70 866.3 | 6.00/ 5.94 ± 0.17 | 128/ −11± 21 | 3.55 | [3]/[4]/[10] |
| | 1 | 72 650.8/ 72 654.3 | 5.29/5.19 | 4.63/−16 | 3.57 | [3]/[4]/[10] |
| | 3 | 75 982.3 | 4.10 | -30 | 3.61 | [10] |
| $f\ ^3\Delta_3[3/2]6p\pi$ | 0 | 64 572.6 | 5.715 | −7.6 | 3.61 | [2] |
| $f\ ^3\Delta_2[3/2]6p\pi$ | 0 | 64 693.9/64 691 | 6.737/6.80 ± 0.03 | 10.6/2.9 ± 1.2 | 3.60 | [3]/[5] |
| | 1 | 66 610 | 6.17± 0.01 | 15± 3 | 3.62 | [5]/[7] |
| $f\ ^3\Delta_1[1/2]6p\pi$ | 0 | 69 687.0/69 699.9 | 6.135/6.31 ± 0.02 | 1.92/4.6 ± 1.0 | 3.62 | [2]/[3]/[4] |
| | 1 | 71 780.5 | 5.957 | 9.73 | 3.62 | [3] |
| $F\ ^1\Delta_2[1/2]6p\pi$ | 0 | 70 228.3/70 223.6 | 6.30/ 6.32 ± 0.01 | 1.2/ 2.6 ± 0.6 | 3.59 | [2]/[3]/[4] |
| | 1 | 72 324.0 | 6.13 | 0.0003 | 3.59 | [6] |
| | 2 | 74 272.8 | 5.93 | 77 | 3.59 | [11] |
| $g\ ^3\Sigma^-_{0+}[3/2]6p\pi$ | 0 | 66 022.6 | 6.110 | 2.5 | 3.51 | [3] |
| | 1 | 67 704.4 | 5.62 | 28 | 3.54 | [3] |
| $g\ ^3\Sigma^-_1{}^{\pm}[1/2]6p\pi$ | 0 | 68 908.8 | 6.06 | 1.7 | 3.67 | [3] |
| $f^3\Delta_2[3/2]7p\pi$ | 0 | 74500.9 | 5.58 | -8.4 | 3.56 | [11] |
| $g\ ^3\Sigma^-_{0+}\ [3/2]7p\pi$ | 0 | 74 735.2 | 6.10 | 14.8 | 3.52 | [8]/[10] |
| | 1 | 76 364.4 | 4.36 | -38 | 3.61 | [10] |
| $g\ ^3\Sigma^-_1{}^{\pm}[1/2]7p\pi$ | 0 | 79 145.1 | 5.77 | 25.9 | 3.68 | [10] |
| $F^1\Delta_2[1/2]7p\pi$ | 0 | 79 923.5 | 6.74 | 10 | 3.54 | [10] |
| **[$\Omega_c$]*n*d$\sigma$ *(n = 5)*** | | | | | | |
| $N\ ^1\Pi_1[1/2]5d\sigma$ | 0 | 71 526.2 | 6.163 | 1.74 | 2.50 | [3] |
| | 2 | 74 899.2 | 6.17 | 6.2 | 2.56 | [8] |
| **[$\Omega_c$]*n*d$\pi$ *(n = 5)*** | | | | | | |
| $H\ ^1\Sigma^+[3/2]5d\pi$ | 0 | 68 277.3 | 5.78 | 5.0 | 2.34 | [3]/[10] |
| | 1 | 70 242.1/70 236.1 | 5.95/6.34 ± 0.01 | 125/1100 ± 20 | 2.36 | [3]/[4]/[10] |
| | 2 | 72 217.6 | 4.35 | 24.2 | 2.36 | [3]/[10] |
| $i\ ^3\Delta_3[3/2]5d\pi$ | 0 | 68 326.2 | 6.21 | −25 | 2.34 | [9] |

| | | | | | | |
|---|---|---|---|---|---|---|
| $I\ ^1\Delta_2[1/2]5d\pi$ | 0 | 71 990/71 989.4 | 6.312/ 6.31 ± 0.01 | 2.7/ 2.4 ± 0.1 | 2.47 | [7]/[4] |
| | 2 | 76 080.8 | 5.82 | 9 | 2.47 | [10] |
| | 3 | 77 954.1 | 5.55 | -2.6 | 2.48 | [10] |
| $j\ ^3\Sigma^-_{0+}[1/2]5d\pi$ | 0 | 73 254.9/73 252.0 | 5.71/5.63 | 47.5/46 | 2.37 | [6] |
| | 1 | 75546.1 | 5.14 | 54.0 | 2.36 | [11] |
| | 2 | 77 346.0 | 5.09 | -79 | 2.37 | [10] |
| $H^1\Sigma^+[3/2]6d\pi$ | 1 | 77 615.4 | 5.56 | 90 | 2.36 | [10] |
| $i^3\Delta_2[3/2]6d\pi$ | 0 | 75 246.1 | 6.14 | 5 | 2.42 | [10] |
| **$[\Omega_c]nd\delta$ (n = 5)** | | | | | | |
| $k\ ^3\Pi_0^{\pm}[3/2]5d\delta$ | 0 | 68 110.7 | 6.24 | 3 | 2.35 | [3] |
| | 1 | 70 320.4/70 310.8 | 5.058/5.13 ± 0.03 | −21/ −4 ± 9 | 2.35 | [3]/[4] |
| | 2 | 72 353.1/72 355.6 | 5.650/5.86 | −5.49/42 | 2.35 | [3] |
| $k\ ^3\Pi_1[3/2]5d\delta$ | 0 | 68 991.8 | 6.459 | 3.3 | 2.28 | [3] |
| | 1 | 71 125.0/71 126.4 | 6.30/6.22 ± 0.02 | 4.82/−2.6 ±1.6 | 2.27 | [3]/[4] |
| | 2 | 73 180.7/73 176.7 | 6.034/6.13 | 8.72/23 | 2.27 | [3] |
| $k\ ^3\Pi_2[1/2]5d\delta$ | 0 | 73 360.9 | 6.403 | 6.123 | 2.36 | [3] |
| | 1 | 75123.0 | 6.26 | 7.9 | 2.39 | [11] |
| $K\ ^1\Pi_1[1/2]5d\delta$ | 0 | 74 282.1 | 6.255 | 6.09 | 2.28 | [3] |
| **$[\Omega_c]nf\pi$ (n = 4,5)** | | | | | | |
| $O\ ^1\Sigma^+[3/2]4f\pi$ | 0 | 71 301.9/71 294.7 | 5.82/ 6.25 ± 0.22 | --/ 33± 26 | 1.04 | [7]/[4] |
| | 1 | 73 383.6/73 384.2 | 5.819/5.70 | 4.46/0 | 1.04 | [3]/[7]/[6] |
| | 2 | 75 410.1 | 5.19 | 38 | 1.04 | [10] |
| | 3 | 77 448.2 | 4.56 | -51 | 1.03 | [10] |
| $p\ ^3\Delta_2[3/2]4f\pi$ | 0 | 73 081.7 | 6.35 | 2.0 | 0.8 | [6]/ [11] |
| $P^1\Delta_2[1/2]4f\pi$ | 0 | 75 124.6 | 6.15 | 8 | 1.20 | [10] |
| | 2 | 78 502.6 | 5.67 | -52 | 1.27 | [10] |
| $q^3\Sigma^-_{0+}[1/2]4f\pi$ | 0 | 76 234.4 | 5.50 | 160 | 1.08 | [10] |

New states.

**Table S5.** Summary of ion-pair states and spectra, previously observed. State specifications, vibrational quantum numbers ($\boldsymbol{v'}= m + i$; $m$ unknown integer), band origin ($\boldsymbol{\nu^0}$), rotational parameters ($\boldsymbol{B'}, \boldsymbol{D'}$) and references.

| State specification | $v'$ [a] | $\nu^0$ /cm$^{-1}$ | $B'$/ cm$^{-1}$ | $D'$*10$^4$ /cm$^{-1}$ | Refs. |
|---|---|---|---|---|---|
| $V\ ^1\Sigma^+_{0+}\ (\sigma\pi^4)\sigma^*$ | $m$ | 68 004.4 | 2.84 | 2.0 | [2]/[3] |
| | $m$+1 | 68 489.4 | 3.3 | -- | [2]/[3] |
| | $m$+2 | 68 927.3 | 3.19 | −1.1 | [2]/[3] |
| | $m$+3 | 69 418.5 | 3.25 | -- | [2]/[3] |
| | $m$+4 | 69 909.9/69 903.3 | 3.273/ 2.94 ± 0.18 | 6.54/ 10± 40 | [2]/[3]/[4] |
| | $m$+5 | 70 512.1/70 511.0 | 3.800/ 3.66 ± 0.02 | −70.2/ 83± 4 | [3]/[4] |
| | $m$+6 | 70 948.6/70 952.3 | 4.09/3.56 ± 0.10 | 44/ 24± 10 | [3]/[4] |
| | $m$+7 | 71 478.4 | 2.95 ± 0.10 | −4 ± 5 | [4] |
| | $m$+8 | 71 920.3/71 924.4 | 3.97/4.17 ± 0.17 | 158/ 270 ± 70 | [3]/[4] |
| | $m$+9 | 72 022.4/72 023.2 | 2.792/2.84 ± 0.03 | −4.61/ 1 ± 4 | [3]/[4] |
| | $m$+10 | 72 506.0/72 508.8 | 4.106/4.25 | 14.7/80 | [3]/[6] |
| | $m$+11 | 72 923.0 | 3.43 | 19 | [6] |
| | $m$+12 | 73 110.8 | 4.34 | 10 | [6] |
| | $m$+13 | 73 457.8/73 459.1 | 3.177/4.52 | −23.7/89 | [3]/[6] |
| | $m$+14 | 73 589.5/73 590.8 | 2.294/2.23 | −11.5/0.0 | [3]/[6] |
| | $m$+15 | 73 822.7/73 831.8 | 3.679/4.14 | −2.25/90 | [3]/[6] |
| | $m$+16 | 74 090.0/74 091.0 | 3.724/3.71 | 5.8/22.6 | [3]/[8] |
| | $m$+17 | 74 372.0 | 3.9 | 4.2 | [8] |
| | $m$+18 | 74 615.4 | 3.76 | 3.67 | [8] |
| | $m$+19 | 74 924.0 | 3.05 | 3.83 | [8] |
| | $m$ + 20 | 75 025.4 | 3.02 | -33 | [10] |
| | $m$ + 21 | 75 189.5 | 2.41 | 1423 | [10] |
| | $m$ + 22 | 75612.6 | 2.80 | 12.0 | [11] |
| | $m$ + 23 | 75 822.0 | 2.79 | 63 | [10] |
| | $m$ + 24 | 75 919.1 | 3.16 | -27 | [10] |
| | $m$ + 26 | 76 479.9 | 2.67 | -31 | [10] |
| | $m$ + 29 | 77 226.8 | 3.13 | 14 | [10] |
| | $m$ + 31 | 77 795.6 | 3.01 | 28 | [10] |

| | | | | | |
|---|---|---|---|---|---|
| | *m* + 32 | 77 934.8 | 2.80 | 11 | [10] |
| | *m* + 35 | 78 585.1 | 2.61 | -54 | [10] |
| | *m* + 36 | 78655.0 | 3.90 | -65.0 | [11] |

a. Vibrational quantum numbers are marked as $v' = m + i$ for positive integer numbers of *i* ranging from zero for the lowest vibrational level observed and *m* as an unknown positive integer.

New states.

## References:

[1] S.G. Tilford, M.L. Ginter, A.M. Bass, *J. Mol. Spectrosc.* 34 (1970) 327.

[2] M.L. Ginter, S.G. Tilford, A.M. Bass, *J. Mol. Spectrosc.* 57 (1975) 271.

[3] D.S. Ginter, M.L. Ginter, S.G. Tilford, *J. Mol. Spectrosc.* 92 (1982) 40.

[4] H. R. Hróðmarsson, H. Wang, and Á. Kvaran, *J. Mol. Spectrosc.* 5 (2013) 290.

[5] S.A. Wright, J.D. McDonald, *J.Chem.Phys.* 101 (1994) 238-245.

[6] H. R. Hróðmarsson, H. Wang, and Á. Kvaran, *J. Chem. Phys.* 142 (2015) 244312.

[7] S.T. Pratt, M.L. Ginter, *J. Chem. Phys.* 102 (1995) 1882-1888.

[8] A. Hafliðason, M-X Jiang and Á, Kvaran, *Phys. Chem. Chem. Phys.* 21 (2019) 23154.

[9] P. M. Regan, D. Ascenzi, E. Wrede, P. A. Cook, M. N. R. Ashfold and A. J. Orr-Ewing, *Phys. Chem. Chem. Phys.* 2 (2000) 23.

[10] M-X. Jiang, A. Hafliðason and Á, Kvaran, *J. Mol. Spectrosc.* 372 (2020) 111329.

[11] This work